Biophysics and Physicobiology

Review Article

Biophysics in oviduct:
Planar cell polarity, cilia, epithelial fold and tube morphogenesis, egg dynamics

Hiroshi Koyama[1,2], Dongbo Shi[1,3,4] and Toshihiko Fujimori[1,2,5]

[1]Division of Embryology, National Institute for Basic Biology, Okazaki, Aichi 444-8787, Japan
[2]SOKENDAI (The Graduate University for Advanced Studies), Okazaki, Aichi 444-8787, Japan
[3]Graduate School of Biostudies, Kyoto University, Kyoto 606-8501, Japan
[4]Centre for Organismal Studies, Heidelberg University, Heidelberg 69120, Germany
[5]CREST, Japan Science and Technology Agency, Kawaguchi, Saitama 332-0012, Japan

Organs and tissues in multi-cellular organisms exhibit various morphologies. Tubular organs have multi-scale morphological features which are closely related to their functions. Here we discuss morphogenesis and the mechanical functions of the vertebrate oviduct in the female reproductive tract, also known as the fallopian tube. The oviduct functions to convey eggs from the ovary to the uterus. In the luminal side of the oviduct, the epithelium forms multiple folds (or ridges) well-aligned along the longitudinal direction of the tube. In the epithelial cells, cilia are formed orienting toward the downstream of the oviduct. The cilia and the folds are supposed to be involved in egg transportation. Planar cell polarity (PCP) is developed in the epithelium, and the disruption of the Celsr1 gene, a PCP related-gene, causes randomization of both cilia and fold orientations, discontinuity of the tube, inefficient egg transportation, and infertility. In this review article, we briefly introduce various biophysical and biomechanical issues in the oviduct, including physical mechanisms of formation of PCP and organized cilia orientation, epithelial cell shape regulation, fold pattern formation generated by mechanical buckling, tubulogenesis, and egg transportation regulated by fluid flow. We also mention about possible roles of the oviducts in egg shape formation and embryogenesis, sinuous patterns of tubes, and fold and tube patterns observed in other tubular organs such as the gut, airways, etc.

Corresponding authors: Hiroshi Koyama, Division of Embryology, National Institute for Basic Biology, 5-1 Higashiyama, Myodaiji, Okazaki, Aichi 444-8787, Japan. e-mail: hkoyama@nibb.ac.jp; Toshihiko Fujimori, Division of Embryology, National Institute for Basic Biology, 5-1 Higashiyama, Myodaiji, Okazaki, Aichi 444-8787, Japan. e-mail: fujimori@nibb.ac.jp

Multi-cellular organisms develop organs and tissues with various three-dimensional morphologies which provide structural basis of their functions. In tubular organs such as the guts, airways, esophagus, oviducts, etc., epithelia form various structures including villi and folds in their luminal sides [1–10]. These structures may be involved in their functions such as nutrient uptake in the guts. In this review, we mainly

◀ *Significance* ▶

The oviduct in the female reproductive tract functions to convey eggs from the ovary to the uterus. To exert this function, alignment of cilia in luminal epithelia, alignment of epithelial folds, and smooth muscle contraction are involved in. Planar cell polarity (PCP) is essential for the formation of some of these structures and also the continuity of the tube. In this review, we discuss how these multiscale structures are formed and how these structures confer the physiological roles of the oviduct. The oviduct is a good model to study multiscale morphogenesis and its contribution to organ physiological roles.
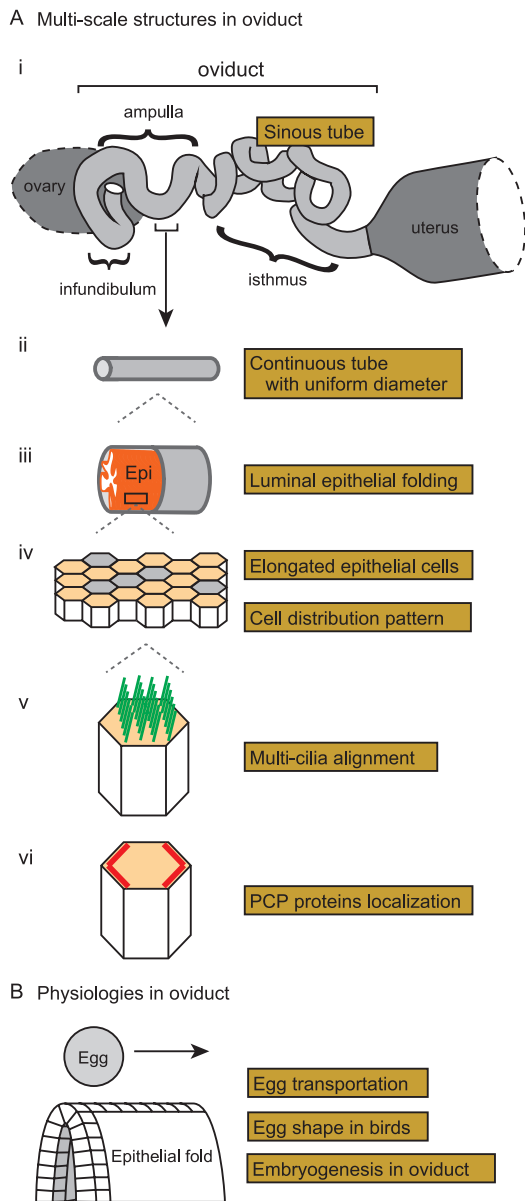
A Multi-scale structures in oviduct

Figure 1 Multi-scale structures and physiologies in murine oviduct. A. Multi-scale structures in the murine oviduct are illustrated. i) A whole view of the oviduct is shown with the three sub-domains: infundibulum, ampulla, and isthmus. The oviduct presents a sinuous tube when the tube is surgically disentangled. Before the surgical operation, the tube is more compactly accommodated as illustrated in Figure 7A. ii) Each sub-domain of the oviduct is a continuous tube with almost uniform diameter. iii) Multiple folds of the luminal epithelia in the infundibulum and ampulla are shown. The epithelial sheet and the surrounding smooth muscle layer are shown by orange and gray, respectively. iv) Cell distribution in the luminal epithelium is shown. The epithelial cells are comprised of ciliated (orange polygons) and secretory (gray polygons) cells, and the formers are elongated along the longitudinal axis of the tube. v) Well-aligned multiple cilia (green lines) in a ciliated cell are shown. vi) Planar cell polarity (PCP) in the luminal epithelium is described. PCP-related proteins (red lines) are localized on specific boundaries of the epithelial cells. B. Physiologies of the mammalian and avian oviducts are illustrated. In the oviducts, eggs are transported along the epithelial folds. Epithelial cells are illustrated as cubic blocks in the fold. Avian egg shapes are determined in the oviduct, which is related to the formation of the anterior-posterior axes of the embryos in the eggs.

focus on the oviduct, a part of the female reproductive tract, also known as the Fallopian tube. The oviduct functions to convey egg from the ovary to the uterus. It is in the oviduct where eggs are fertilized with sperms. The fertilized eggs undergo their development to form blastocysts before arriving at the uterus in mammals. A mammalian oviduct is typically divided into three sub-domains from the ovary to the uterus: infundibulum, ampulla, and isthmus (Fig. 1A-i). In the infundibulum and ampulla, the luminal epithelia form multiple folds aligned along the longitudinal direction of the oviduct (Fig. 1A-iii) [1,11,12]. The epithelia are occupied by ciliated cells especially in the infundibulum and the ampulla, on which cilia are beating toward the direction along the ovary to the uterus (Fig. 1A-v) [11,13]. Both the cilia and the folds may contribute to the transportation of the eggs, which will be mentioned in later sections [11].

Developments of the cilia and the folds in the oviduct are regulated by planar cell polarity (PCP), which is one of the most important directional information by which tissue level polarities are established and sub-cellular structures including cilia are correctly oriented [14]. PCP was originally discovered in wing cells of Drosophila, and many proteins essential for PCP establishment have been found including Flamingo, Vang, etc. [15,16]. These proteins, called core PCP proteins, are localized on specific boundaries of epithelial cellular edges, which is linked to tissue level polarities [17–19]. How the core PCP proteins are correctly localized is not fully understood and will be discussed in later sections. In the oviduct, Celsr1 proteins, a mammalian homolog of Flamingo, are localized on specific boundaries of the luminal epithelial cells, presenting PCP (Fig. 1A-vi) [11,20]. We found that, in Celsr1 mutant mice, cilia are formed but their orientations are randomized (Fig. 3C) [11]. Furthermore, in the mutants, the orientations of the epithelial folds are also randomized with ectopic branches (Fig. 4C), and the tube of the oviduct is stochastically narrowed down or shows discontinuities (Fig. 1A-ii and 6B) [11]. Thus, the multi-scale structures in the oviduct are regulated by PCP and the related proteins. Moreover, the mutants show inefficiency of egg transportation and are infertile [11], suggesting the involvement of the multi-scale structures in the functions of the oviduct.

In this review, we discuss biophysical and biomechanical aspects related to the oviducts. Since the oviducts have not been studied well in biophysical and developmental biology fields, we intend to review wide-range of topics in the oviducts, including morphogenesis and pattern formation of the multi-scale structures (Fig. 1A), and their physiological roles in egg transportation and embryogenesis (Fig. 1B). Furthermore, to clarify the generalities and specificities of the oviducts, we compare the mouse oviduct with the oviducts in other species such as birds and with other tubular organs such as the airways and guts.
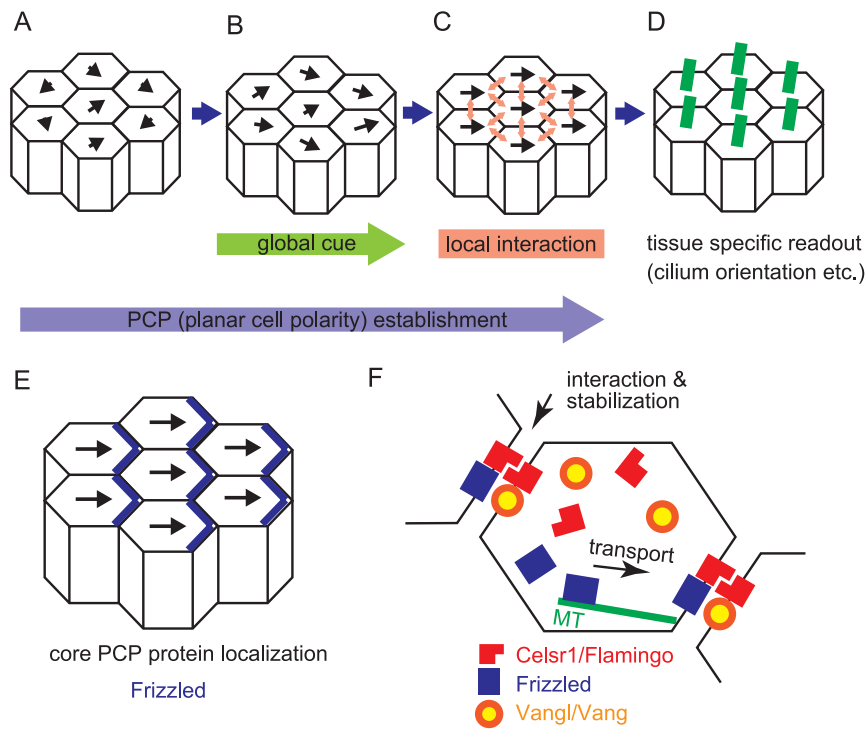
Figure 2 Formation of planar cell polarity. A–D. Establishment of planar cell polarity (PCP) is illustrated according to the three-tiered model. Epithelial cells are shown by polygons, and their polarities are described by black arrows. The lengths of the arrows mean the strengths of the polarities. A. Before the establishment, epithelial cells have weak polarities with randomized directions. B. The polarities in the epithelial cells in the presence of a global directional cue are shown. C. The polarities in the presence of local signal propagation are shown. Between adjacent cells, local signals are transduced (light red arrows). Consequently, all epithelial cells exhibit almost the same direction of the polarities. D. Tissue specific readout of PCP established in C includes cilium orientation etc. Cilia are exemplified. They are described by green lines, and orient toward right sides of the cells in this panel. E. A relationship between the directions of the cellular polarities and localization of core PCP proteins is illustrated. The localization of Frizzled proteins is exemplified (blue lines). F. Molecular mechanisms of PCP establishment are described. The epithelial cells are shown by polygons. Several core PCP proteins are shown by red, blue, and orange/yellow. These proteins are located on specific boundaries of the cells. On the cellular boundaries, these proteins might form complexes with proteins from neighboring cells, which contributes to the stabilization of the localization. Some of core PCP proteins are transported to the specific boundaries along microtubules (green lines). In the oviduct, the Celsr1 proteins are localized on the boundaries of both the ovary and the uterus sides, whereas the Vangl proteins are localized on the boundaries of the ovary side.

Planar Cell Polarity (PCP) Pathway

Cells are the basic building block for organisms to form their body. Unlike 3D-printers where the materials are deposited according to the absolute coordinates, cells have to know the right direction by themselves to migrate, proliferate, and polarize, etc. for the appropriate morphogenesis. PCP pathway is used as an efficient and accurate way to orchestrate the direction information among cells in various species [14]. A three-tiered model is proposed for the PCP pathway function based on analyses in fly wing cells (Fig. 2A–D) [21]. In this model, a group of proteins function in generating 1) global cues which directs the polarity vector of each cell like a magnetic field (Fig. 2B), 2) signal propagation via local interactions with feedback loop which orchestrates the vector between neighbor cells (Fig. 2C), and 3) tissue specific readout which forms sub-cellular structure such as cilia according to the vector (Fig. 2D), respectively.

One of the key features of the PCP pathway is that a group of proteins called "core PCP protein" shows a polarized localization in each cell (Fig. 2E) [22,23]. This polarized localization is important for the signal propagation among cells via the intercellular core PCP protein–protein interaction. When any of these core PCP genes are mutated in fly, randomized PCP phenotypes are observed in the wing together with mis-localization of other core PCP proteins, suggesting that these core PCP proteins function together. Through mosaic analyses with ectopic gene expression or down regulation, it is found that one type of protein complex (Flamingo-Frizzled-Dishevelled, for example) in one cellular edge can recruit the other type of protein complex (Flamingo-Vang-Prickle) to the contacting cellular edge of the neighboring cells (Fig. 2F) [24,25]. The direction of protein polarization is regarded as a vector of cellular polarity (Fig. 2E), and therefore, the chain reaction of these intercellular protein complex recruitment is able to explain tissue-level PCP propagation. Flamingo belongs to cadherin-super families and is thought to function in intercellular interaction

through its property of intercellular homophilic adhesion (Fig. 2F). These interaction networks correspond to the second step in the three-tiered model mentioned above (Fig. 2C). In mouse oviduct, several core PCP proteins, including a mammalian Flamingo homologue Celsr1, mammalian Vang homologues Vangl1/2, and Frizzled 6, are asymmetrically localized at cellular boundary (Fig. 2F) [11,20]. Disruption of the Celsr1 gene causes mis-localization of other PCP proteins [11]. How these asymmetries are generated and maintained is a common interest of this field. One of the current models proposes that the gradient of upstream gene expression caused polarized transport of core PCP proteins on microtubules in each cell (Fig. 2F), and this asymmetrical localization is strengthened by intercellular core PCP protein–protein interaction [26–29]. This upstream regulation corresponds to the first step in the three-tiered model (Fig. 2B). However, more and more factors are found to be regulating this process [30–32], and the underlying mechanisms can be different in various tissues. In the oviducts, the upstream regulators have not been identified yet.

It is also suggested that the polarized transport of core PCP proteins on microtubules is not required for the maintenance of polarized localization of core PCP [20,23,33], thus there might be additional mechanism to maintain this asymmetry. By performing fluorescence recovery after photobleaching (FRAP) analysis, it is shown that core PCP proteins in enriched cellular edges have stronger stability compared to that in less-enriched cellular edges, suggesting the core PCP proteins might form more stable structure in enriched cellular edges (Fig. 2F) [20,34,35]. So far, the mechanism for regulating the stability of core PCP proteins is unknown. Since cytoskeletal proteins such as Septins are known to function together with PCP pathway [36,37], this mechanism might also be cytoskeletal related. General open questions related to PCP formation have been reviewed in other papers [14,23–25].

Mathematical modeling and simulations together with genetic perturbation are used to dissect the underling mechanisms and how the first and second tiers are linked to form the polarity [38–41]. These mathematical models consider local rules between neighboring cells and global cues. The local rules are implemented on the basis of the dynamics of the core PCP proteins or of a vector for each cell. In the former cases, the local rules are modeled by reactions of protein–protein association and dissociation on cell-cell boundaries [38,39,41]. Diffusions of these proteins and the protein complexes are also considered. In the latter cases, a vector is assumed for each cell, which is also called "PCP nematic" in analogy to liquid crystals, and the local rules are modeled to align the vector/PCP nematic between neighboring cells [40]. Simulations based on these two cases successfully explain the observed vector field in several conditions corresponding to mutant or chimeric tissues.

In the models based on the dynamics of the core PCP proteins, the reactions and diffusions are biochemically and physically well-defined processes [38,39]. Global cues are modeled to modify the rates of the reactions in an intracellular position dependent manner. However, biochemical or physical bases of how the global cues modify the local reactions remain unknown. In more macroscopic models such as the cellular vector-based model, it is established that tissue deformation is involved in tissue level alignment of the cellular vectors [40,41]. Cell proliferation is also effective for tissue level alignment of cellular vectors [41]. In comparison with bacterial cells and migrating cells which can also align their vectors through their self-propelled abilities [42–44], tissue deformation or cell proliferation maintains the systems under far-from-equilibrium states by actively moving the cells, which might have an effect similar to the self-propelled abilities. As mentioned in later sections, PCP has a critical role in tissue morphogenesis. Taken together, PCP formation and tissue deformation can form a feedback loop, and it will be investigated whether such feedback systems contribute to morphogenesis and ensure consistency between complicated three-dimensional tissue morphologies and directions of PCP. In particular, during the development of the oviducts, the sinuous patterns of the tubes are enhanced and the epithelial folds are newly generated to form a curved sheet, indicating a dynamics change in the morphologies of the epithelia. It has not been studied how PCP is correctly formed under such environment or whether the three-dimensional changes in the morphologies positively or negatively influence the correct formation of PCP.

Orchestrating Cilia Polarity and Distribution of Ciliated Cells

The inner lumen of the oviducts is covered with asymmetric motile cilia, which is sufficient to transport the ovum towards the uterus [13,45]. In the infundibulum, the epithelia are largely occupied by the ciliated cells (~80% in adult mice) [11]. The population becomes less in the isthmus. Hundreds of cilia are localized in one ciliated cell and each cilium has a structural asymmetry corresponding to the asymmetric mobility (Fig. 3B). During development, these cilia are initially randomly deposited to the apical surface of cells, and then they become aligned with orchestrated orientation afterwards (Fig. 3A and B) [46]. In Celsr1 deficient mice, multi-ciliated cells are generated but the cilia are not well aligned and their orientations of cilia are randomized (Fig. 3C). How to orchestrate these dense and tiny structures (about 6 cilia per μm^2) into a well aligned array towards a single orientation is still a mystery. Experimental studies have revealed that cytoskeletal networks of actin and microtubules are linking the base of cilia (basal body) at the apical surface of cells, and these networks are required for appropriate ciliary alignment and polarity coordination (Fig. 3D) [47,48]. In addition, PCP pathway and a part of ciliary structure called "basal foot" are required for the polarity
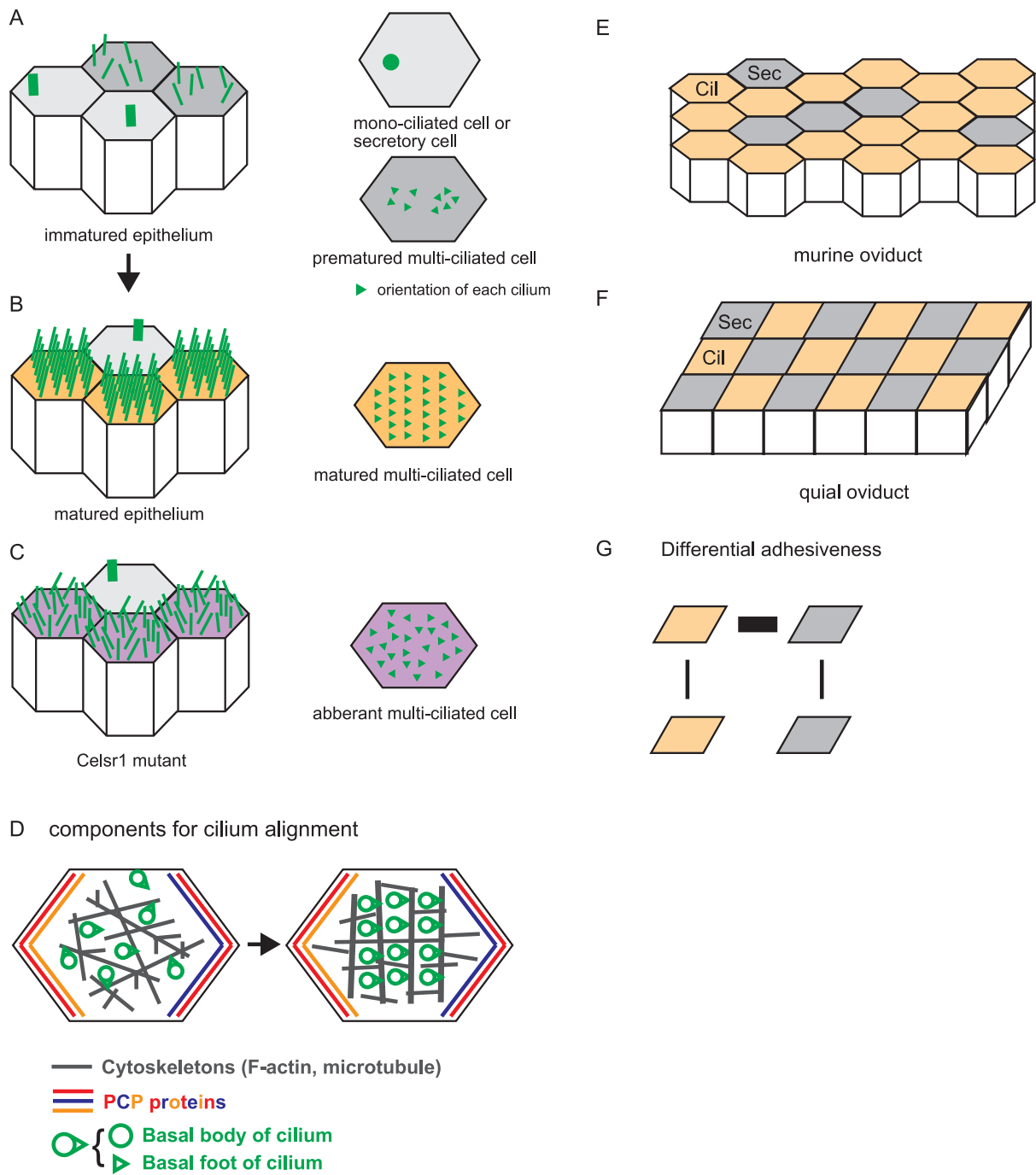
Figure 3 Alignment of multiple cilia in a single cell and a tissue, and distribution of ciliated cells. A. An immature epithelium is illustrated with cilia. Cells are depicted as polygons, and each cilium is shown by a green line (left panel). There are mono-ciliated cells and premature multi-ciliated cells as shown in the right panel where cilia are described as green triangles whose orientations are randomized. B. A mature epithelium is illustrated with cilia. The cilia are ordered, and their orientations are aligned in multi-ciliated cells. Mono-ciliated cells are also observed. C. A mature epithelium in the Celsr1 mutant mice is illustrated with cilia. The cilia are not ordered, and their orientations are not aligned in multi-ciliated cells. D. Components involved in cilium alignment and the process of cilium alignment are described. A single epithelial cell is shown by a polygon. Basal bodies and basal foots of cilia are depicted by green circles and triangles, respectively. Cytoskeletons are shown by gray. Localization of the core PCP proteins are shown by red, blue, and orange. Cilia become aligned with the cooperation of cytoskeletal filaments (from left to right panel). E. A murine oviduct epithelium is shown. Ciliated and secretory cells are described by orange polygons (Cil) and gray polygons (Sec), respectively. Three secretory cells align linearly in this panel. F. A quail epithelium is shown. Ciliated (Cil) and secretory (Sec) cells form a checkerboard pattern. G. Differential adhesion hypothesis (DAH). According to DAH, the checkerboard pattern in the quail oviducts is explained by differential adhesiveness between each pair of the cells (Cil and Sec). Thicknesses of black lines connecting the cells mean the strengths of cell-cell adhesion.

coordination (Fig. 3D) [11,49–52], and external mechanical fluid flow and mechanical strain applied to tissues can also orchestrate the ciliary polarity [35,53,54].

The development of multi ciliated cells can also be observed in cultured tracheal cells [55], where researchers are able to analyze the process in more detail. The alignment of cilia (or basal bodies) is correlated with the orchestrated orientation of cilia, and both alignment and orchestrated orientation are dependent on microtubules (Fig. 3D) [48]. Theoretical studies revealed that, given that basal body is associated with the cytoskeletons through their basal foot and are transported by active cytoskeletal flows, mathematical simulations could recapitulate the development of ciliary alignment based on active hydrodynamic theories [48,56,57]. The active cytoskeletal flows are generated by polymerization/depolymerization and motor-induced remodeling of the cytoskeletal network, etc.[48], suggesting that self-organizing properties of microtubules are critical for ciliary alignment. Although ciliary alignment was successfully reproduced in the simulations, ciliary orientation was not considered. How ciliary orientation is regulated and how the localized PCP proteins are involved in the process are under investigation.

For the functional transport of eggs, the phase of ciliary beating should also be orchestrated. Analysis in the oviducts revealed that the beating frequency is maintained in local level [13]. The precise mechanism for the frequency or phase orchestration is unknown, but hydrodynamical simulations predict that the neighboring cilia can synchronize autonomously by the hydrodynamics of moving cilia and fluid [58–60]. Thus, the cilia should be positioned closely enough to mechanically influence each other, and the overall distribution pattern of the cilia will be important for the transport.

For efficient transport of eggs, tissue level spatial distribution of ciliated cells can be effective. In the mouse oviducts, the ciliated cells and secretory cells are major population of epithelial cells, and the formers largely occupy the epithelia in the infundibulum and probably in the ampulla [11]. In mice, smaller populations of the secretory cells are distributed almost randomly or sometimes formed a small cluster with linearly aligned (Fig. 3E) [11]. By contrast, the ciliated cells and the secretory cells are beautifully arranged in a checkerboard pattern in the adult quail oviducts (Fig. 3F) [61]. These two cell types originate from the same precursors. Immediately after the hatching from the egg, cell differentiation to these two cell types is not evident, and the boundaries between cells are zigzag like a jigsaw puzzle. Once the ciliated cells differentiate, the ciliated cells are surrounded by the secretory cells in a random polygonal pattern. Along the maturation of the animals, the number of the ciliated cells increases, and the ciliated cells and the secretory cells are arranged in a checkerboard pattern [61]. These changes in cell arrangement suggest differential adhesion between the cell types (Fig. 3G) [62,63], and the maximum mechanical adhesion should be between the ciliated and the secretory cells. The mechanism by which two types of cells

are arranged in a checkerboard pattern was studied in other tissues. An example of this type of cell arrangement based on differential cell adhesion mediated by Cadherin and Nectin was reported in auditory epithelium of mice [64]. The distribution patterns of the ciliated cells could influence the overall efficiency of cilia beating. Because this checkerboard pattern is seen in magnum of quails where the egg white is secreted, it might be advantageous to efficiently transport the egg and simultaneously cover the yolk with the egg white. In comparison between birds and mice, the organized spatial distribution patterns in birds might be evolved to transport larger eggs. However, the effects of both spatial distribution of the ciliated cells and the density/alignment of cilia in each ciliated cell on efficient egg transportation have not been evaluated yet.

How are Luminal Fold Patterns Generated?

In tubular organs, luminal epithelia often exhibit various fold patterns or villi. In the guts, circumferential folds as well as the villi are formed [2,65]. Folds are observed in the oviducts, airways, esophagus, stomach etc., and the fold patterns include longitudinally-aligned, randomized, zigzag, etc [1–10]. Honey comb and spiral patterns are also observed in some species [66–70]. Epithelial folding occurs not only in tubular organs but also in other types of tissues/organs such as the brains and early embryos [71–75], suggesting that the folding is a general principle of morphogenesis of multi-cellular organisms.

Mechanical buckling is a well-known concept for folding. When a plane elastic sheet is pushed inward from its boundaries, some parts of the sheet get higher, resulting in the formation of folds (or ridges) (Fig. 4A). The patterns and the number of the folds generated are dependent on stiffness of the sheet and direction of pushing forces [3,6,12,70,76]. A cell sheet growing through cell proliferation can actively push surrounding spatial constraints and forms folds. Theoretical studies based on buckling have been performed and successfully generated various patterns of folds such as longitudinal, circumferential, labyrinths, villi etc. [3,4,6,12,77–80]. On the other hands, reaction-diffusion systems based on chemical signaling are also candidates for the generation of complicated patterns of folds [65]. However, there are a few studies with sound experimental validations for these hypotheses.

In the oviducts, longitudinally well-aligned folds are formed in the luminal side (Fig. 4B), which is widely conserved among various species including mice, birds, reptiles, amphibians, and likely humans [1,81–84]. In contrast, in the Celsr1 deficient mice, the folds showed randomized directions with ectopic branches in the infundibulum (Fig. 4C) [11]. The folds are composed of a single-layered luminal epithelial sheet surrounded by a thick smooth muscle layer (Fig. 4F) [12]. Between these layers, mesenchymal cells form a thin layer. These histological observations are import-
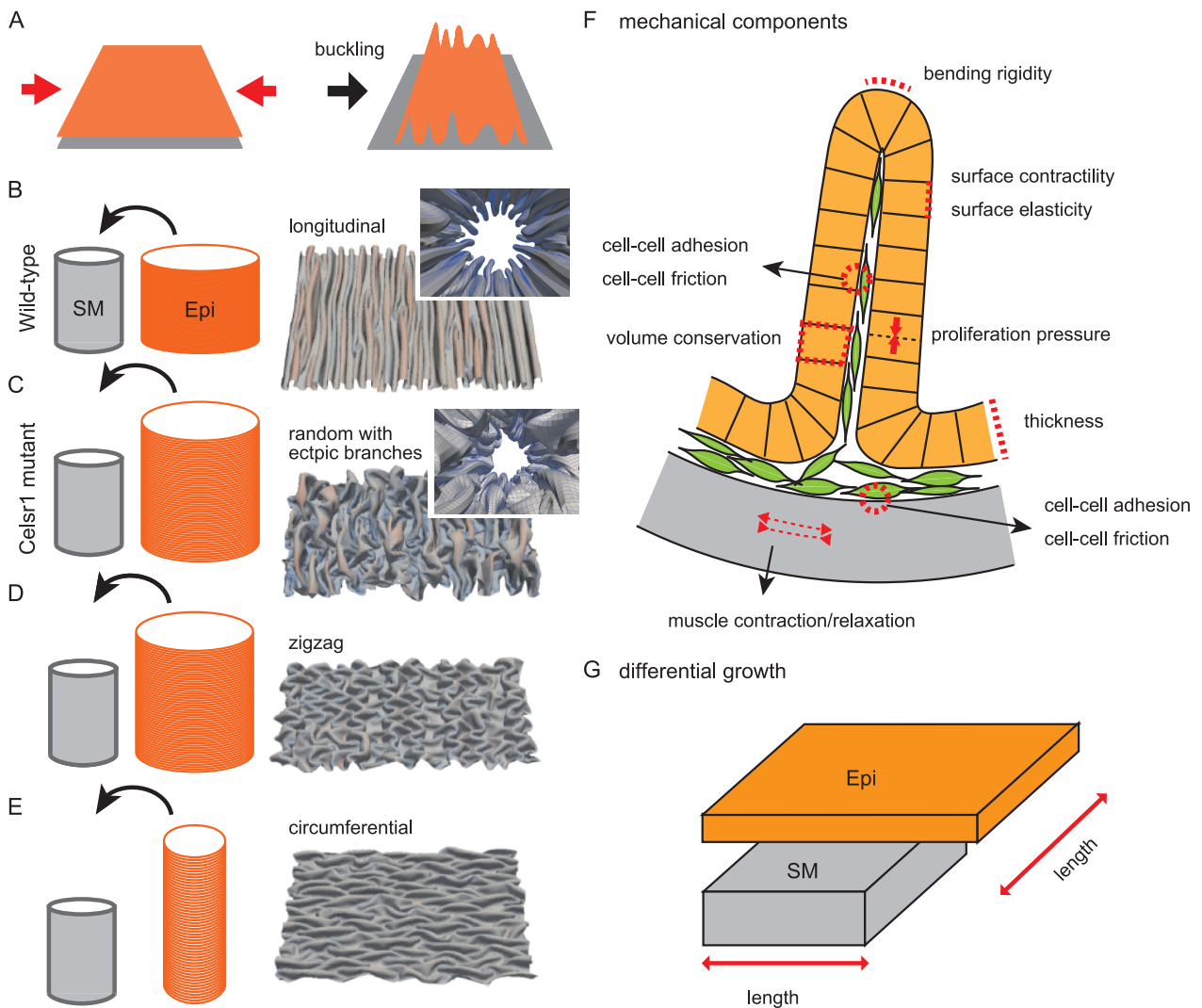
Figure 4   Pattern formation of multiple folds. A. Buckling is explained. When an elastic sheet such as an epithelium (orange) is pushed inward (red arrows), folds are formed. B. Folding in wild-type situations is illustrated. A cylindrical epithelial sheet (orange; Epi) is put into a cylindrical smooth muscle layer (gray, SM). The circumferential length of the Epi is longer than that of the SM, whereas the longitudinal length is comparable. A luminal view with folds generated in our simulation is shown in the inset of the right panel. An opened view of the luminal side is also shown where longitudinal multiple folds are observed. C. Folding in Celsr1 mutant situations is illustrated. In contrast to the wild-type situation (B), the longitudinal length of the Epi is longer than that of the SM. The generated folds exhibit randomized directions with ectopic branches. D. Generation of zigzag folds is explained. The lengths of the Epi and SM are similar to those in C, but the outcomes can be different due to the initial condition of the simulations. E. Generation of circumferential folds is explained. The circumferential lengths of the two layers are comparable, whereas the longitudinal length of the Epi is longer than that of the SM. F. Mechanical components potentially related to fold patterns are described. A circumferential section of the oviduct is shown. An epithelial sheet (orange) forming a fold is shown with each cell (orange box). A smooth muscle layer is shown by gray. Mesenchymal cells are also shown by green. Many potential components can be considered, but we implemented only several components in our simulation explaining the fold patterns [12]. G. Differential growth or length between an epithelial sheet (Epi) and a smooth muscle layer is described. The simulation results (B-E) are cited from our previous work [12].

ant to hypothesize which structures are effective on the generation and the pattern formation of the folds. We can assume various mechanical components as described in Figure 4F. In our previous study, we considered minimal components including elastic properties of the epithelial layer, thickness of the epithelial layer, spatial constraints provided from the smooth muscle layer, and length differences between the epithelial and the smooth muscle layers (Fig. 4B, C, F, and G) [12]. This minimal model was able to recapitulate the

fold patterns observed in both the wild-type and the Celsr1 deficient mice [12]. When the epithelial layers were assumed to be longer than the smooth muscle layer along the circumferential direction, mechanical buckling occurred, resulting in the formation of longitudinally directed folds as observed in the wild-type mice (Fig. 4B). In addition to the circumferential length, if the longitudinal length of the epithelial layer was assumed to be longer than that of the smooth muscle layer, then randomized folds with ectopic branches were

formed as observed in the Celsr1 mutant mice (Fig. 4C). The relative lengths of the epithelial layers in the simulations were consistent with those calculated *in vivo*. Furthermore, epithelial tensions predicted from the simulations were consistent with the *in vivo* values measured by performing laser ablation experiments. In addition, during ovulation, the tubes were diluted and the fold shapes and heights were altered, suggesting that fold shapes are mechanically determined. Thus, mechanical buckling would be responsible for the generation and the pattern formation of the folds in the oviducts. How the lengths or growths of the epithelial layers are regulated is an important question (Figs. 4G and 8A), and we will discuss with the relation to Celsr1 in a later section "Cell elongation and tissue length regulation".

Longitudinally-well aligned folds in the oviducts are also observed in other species such as birds and frogs [70,81–83]. In the chicken or quails, each fold is extremely larger than that in mice; millimeter order vs. several tens micrometer order in the thickness. The folds in the birds may be composed of a stratified epithelial and a thick mesenchymal layers. Although the folds in mice and birds are different in their size and in histology, the similar fold patterns are generated, implying the general roles of the folds in the oviducts.

In the guts, villi are observed in the luminal side [2,65]. During the development of the villi in the chicks, longitudinally-aligned folds are formed and then they are subsequently changed in zigzag folds, and finally changed into the villi [2]. The longitudinally-aligned folds are generated by buckling along the circumferential direction. The zigzag folds are generated by buckling along the longitudinal direction, which are provoked by longitudinally directed constriction of the smooth muscle layer [2,9]. Although both the zigzag folds in the guts and the randomized folds in the Celsr1 deficient oviducts result from longitudinally directed buckling, the outcomes of the fold patterns are different (Fig. 4C and D) [70]. This difference is derived from the initial shapes of the folds before longitudinal buckling occurs: longitudinally-aligned folds are the prerequisite for the generation of the zigzag patterns, whereas a simultaneous buckling along the longitudinally and circumferentially directions occurs in a plane sheet for the generation of the randomized folds as shown in our previous study [12]. In addition, longitudinally directed buckling alone causes generation of circumferential folds which are observed in the intestines (Fig. 4E) [12]. When the villi are formed from the zigzag folds, cell proliferations are locally activated, which depends on the geometric information of the folds [2]. In the mouse gut, the positions of the villi are determined by reaction-diffusion systems based on chemical signaling without experiencing fold formation [65]. In addition, mechanical buckling alone can theoretically generate villi [79]. Taken together, epithelial fold patterns can be regulated by mechanical buckling, chemical signaling, and developmental processes.

Another mechanism for folding is based on apical constriction. If apical surface of epithelia is locally constricted by apical actomyosin activation, the region is invaginated toward the basal direction. These phenomena are often observed during early embryogenesis [72,75,85,86]. To generate a deeper valley or a higher fold, not only apical constriction but also the increase in the length of the epithelial sheet would be required, which can be achieved by cell proliferation etc [70]. Apical constriction-based mechanism can strictly determine the position of folding, whereas buckling-based one cannot do because folding occurs by chance. The width and the number of the folds are almost determined even in the buckling-based mechanism; thickness and bending rigidity of the sheet are effective on the width and the number (Fig. 4F and G) [3,6,12]. Since ciliated cells and secretory cells in the epithelia may be mechanically different, mechanical properties of the epithelia should become non-uniform, which might also affect the position of folding. In the tubular organs, it is unknown whether fold positions should be strictly determined to exert their functions. How the folds in the oviduct contribute to egg transportation will be discussed in the later section, "Egg transportation". To evaluate the physiological meaning of fold positions, further identification of genes which are involved in fold patterns are required. Techniques to artificially modify fold patterns are also useful, though there have been no application except for *in vitro* [87].

Cell Elongation and Tissue Length Regulation

Epithelial cells exhibit various shapes which can be related to morphogenesis of their tissues/organs [88,89]. An epithelial cell typically shows a polygonal shape on its apical surface, which has around five to seven vertices [90,91]. An epithelial cell also shows an elongated shape in its apical surface especially during morphogenesis of the tissue [92,93]. In general, these cells become rounded due to their surface tensions if they are isolated from their tissues. Cell elongation can be achieved by two different ways: cell-autonomous/active deformation and non-cell-autonomous/passive deformation. If cells actively elongate, the generated mechanical forces can deform the tissue. The examples include the elongation of the notochord, the tracheal tube in Drosophila etc [94,95]. In contrast, if a tissue is passively deformed by extrinsic mechanical forces, the composed cells can be also passively elongated. The examples include cells in wing disks in Drosophila and the mouse notochord etc [41,96]. Thus, cell elongation is important information to understand mechanics in morphogenesis of tissues.

In the mouse oviducts, the epithelial cells are elongated along the longitudinal direction of the tube not only during morphogenesis but also in the adult stages (Fig. 5A) [11]. By contrast, in the Celsr1 mutant oviducts, the epithelial cells are less elongated and the orientations are randomized (Fig. 5A) [11]. Whether does Celsr1 primarily regulate the

cell elongation or the epithelial fold patterns? Our mosaic analyses using chimeric mice revealed that wild-type cells are correctly elongated even when they are surrounded by the mutant cells [11]. Since the wild-type and mutant cells should share similar extrinsic environment in the chimeric oviducts, it is supposed that the wild-type cells have an intrinsic feature to elongate.

In the case that the epithelial cells have an intrinsic feature to elongate along the longitudinal direction of the tube, the epithelial sheet may also elongate along the same direction (Fig. 5B, left panel) [95]. However, since the longitudinal elongation of the sheet should result in the increase in the relative length of the sheet compared to the smooth muscle layer, the directions of the folds would be randomized in the wild-type, which is inconsistent with the *in vivo* situations. On the other hand, there is a case where the direction of tissue elongation is not correlated with that of cell elongation: during convergent extension of tissues, the tissue will shrink along the direction of cell elongation, which is achieved by cell-cell junctional remodeling (Fig. 5B, right panel) [94]. Thus, we suppose that cell-cell junctional remodeling occurs in the wild-type oviducts to prevent the epithelial sheet from longitudinally elongating (Fig. 5B, right panel) [12], though this idea has not been validated due to technical limitation of live imaging.

Epithelial tensions can be also related to the lengths of the epithelial sheet. In our study, the epithelial tensions along the longitudinal direction were increased in the wild-type oviducts compared to those in the Celsr1 mutant oviducts (Fig. 5A) [12]. This relationship was reproduced in our simulations. Epithelial tensions would be largely dependent on cell-cell boundary tensions which are generated by actomyosins [97]. However, the difference in the epithelial tensions between the two genotypes was not derived from each cell-cell boundary tension but from epithelial cell arrays (Fig. 5A). In the cell arrays with longitudinally elongated cells observed in the wild-type, larger number of cell-cell boundaries can contribute to the increase in epithelial tensions [12]. Since increased epithelial tensions would work to shrink the length of the sheet, active cell elongation can be involved in the regulation of epithelial tensions and subsequent epithelial lengths. The PCP pathway generates directional differences of epithelial cells. Downstream of this pathway includes activation of actomyosin which is the most fundamental component to provide mechanical properties of cells [75,98]. In addition, some of the core PCP factors such as Celsr1 are a member of cadherin-superfamilies, implying their involvement in cell-cell adhesion. These functions can be closely related to mechanical properties of cell-cell boundaries [99], and subsequent cell-cell junctional remodeling. To understand the mechanism of how Celsr1 regulates the lengths of the epithelial sheet, further analyses of cellular dynamics including cell-cell boundary tensions as well as cell-cell junctional remodeling are required through the developmental process of the oviducts.
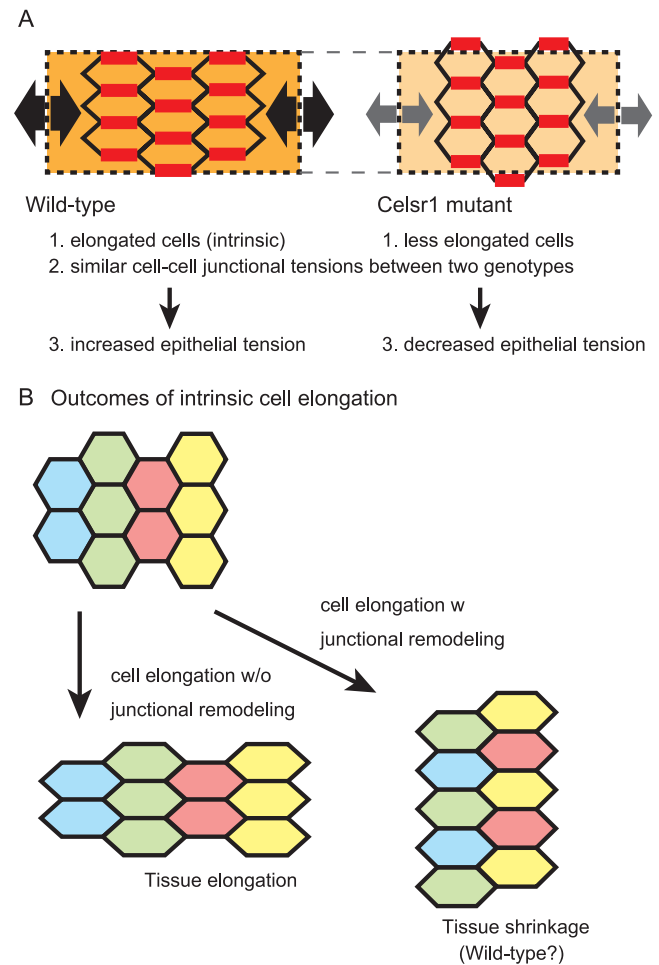

Figure 5 Cell elongation and tissue length regulation. A. Epithelial cell elongation is illustrated in the wild-type and Celar1 mutant situations. In the wild-type, the cells are intrinsically elongated along the longitudinal direction of the tube. Cell-cell junctional tensions are almost similar between the two genotypes (red lines). Combination of the elongated shapes of the cells and the cell-cell junctional tensions results in increased epithelial tension in the wild-type compared to that in the mutant (black and gray arrows). B. Outcomes of intrinsic cell elongation are explained. In the absence of junctional remodeling, the tissue is also elongated. By contrast, in the presence of junctional remodeling, the tissue can be shrunk.

Regulation of tissue length is fundamental for various morphogenesis as well as in the generation of the folds of the oviducts [95,100,101]. In the kidneys, PCP proteins regulate the growth of the renal tubules [101]. As we will mention in a later section, the formation of sinuous patterns of the tubular organs such as the guts is regulated by the differential growth rate of two adjacent tissues [102,103]. Cell proliferation rate and cell division orientation can influence growth rate and its direction of tissues. In the oviducts, we could not detect significant differences in these parameters between the wild-type and the Celsr1 mutant mice [11]. Lateral mechanical stress in epithelial layer can be also involved in the regulation of tissue lengths. In the presence of geometric constraints such as the smooth muscle layer in the case of

the oviducts, increased cell density in epithelia changes mechanical environments or lateral stress, whose information can be transduced to cell proliferation rate or live cell delamination [104–107]. This kind of feedback systems from surrounding environments or states of epithelial cells can be powerful to accurately control tissue lengths, though this idea has not been mathematical/theoretical investigated. Probability of cell-cell junctional remodeling might be also included in these feedback systems. To implement these systems, mechano-sensitive machineries including mechano-sensor molecules are required [108–110]. All mechanisms mentioned above are largely dependent on cell properties of each tissue. Thus, analyzing cell properties and subsequent mathematical simulations are necessary to understand regulation of tissue lengths.

Continuous Tube with Uniform Diameter

To develop a continuous tube with a uniform diameter is essential to confer the function of the tubular organs [95,101]. The oviduct is a tube with a uniform diameter in each segment such as the ampulla and the isthmus (Fig. 6A), but in the Celsr1 mutant mice, the lumen of the tube is stochastically closed, resulting in the loss of the continuity of the tube (Fig. 6B) [11,111]. A theoretical study suggested that, when an epithelial sheet is relatively stiff, differential growth between the epithelial sheet and the surrounding tissue can mechanically cause the formation of a tube with non-uniform diameter [112] or a tube with sinuous patterns as discussed in a later section "Sinuous patterns of tubular organs". In these cases, a soft tissue comprised of extra-cellular matrix is assumed as the surrounding tissue. Thus, the excess growth of the epithelial sheet can deform the surrounding tissue (Fig. 8B). Importantly, no stiff tissues such as a smooth muscle layer are assumed.

In the case of the oviducts, however, the surrounding tissues of the epithelial layers contain the smooth muscle layers which are much larger than the epithelial layers. Furthermore, the phenotype of the Celsr1 mutant mice is quite severe compared with the theoretical result: the discontinuity of the tubes is observed in the Celsr1 mutant mice (Fig. 6B, bottom panel) [11] but not in the theoretical analyses [112]. One possibility is that the tubes in the mutants deformed to have non-uniform diameters at the early stage of the development when the surrounding tissues are still not so stiff, and this aberrant deformation is enhanced during the later developmental processes.

Another possibility is that the discontinuity is derived from the defect of epithelium formation in the mutants. In mutant mice of Vangl2 which is another member of PCP pathway, the female reproductive tissues shows (pseudo)-stratified epithelium and abnormal localization of cytoskeletal components [111]. During development, cells of the coelomic epithelium invaginate and migrate along Wolfian duct in a rostral to caudal manner, forming female reproductive duct
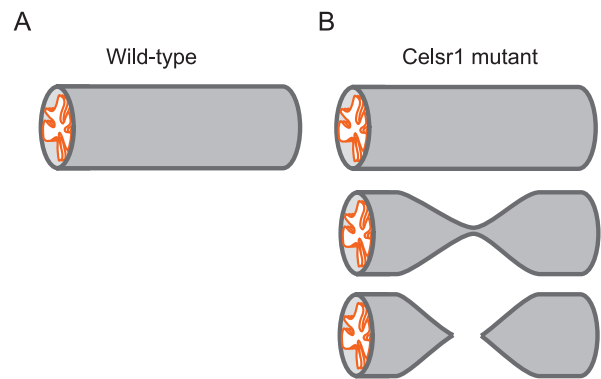

Figure 6 Continuity and uniformity of tubular organ. A. A wild-type oviduct is illustrated which is continuous with uniform diameters. B. Celsr1 mutant oviducts are illustrated. Normal tubes similar to the wild-type are observed (top panel), but the tubes are stochastically narrowed (middle panel), or the continuities are lost (bottom panel).

(or Müllerian duct) [113,114]. Gene expression analysis suggests that cells forming Müllerian duct cells are initially mesenchymal cells and transit into epithelial cells in later stage [20,111,114]. Thus, the discontinuity of female reproductive duct might be caused by the malfunction of this mesenchymal-to-epithelial transition, and an epithelial tube is not accordingly formed or maintained. Anyway, histological observations or live imaging during early stage of the development in the mutant mice are required to examine these hypotheses.

Sinuous Patterns of Tubular Organs

Tubular organs including the oviducts, the murine epididymal tubes, and the guts show sinuous patterns of the tubes (Fig. 7A and B) [11,102,115]. Because the lengths of these tubes are very long, the sinuous patterns would be essential to compactly accommodate these tubes in the bodies (Fig. 7A). There are at least two mechanisms to generate the sinuous patterns. The first depends on the relative stiffness between the epithelial sheet and the tube itself. The second depends on membranes connecting tubes such as the mesenteric membrane for the guts. These two mechanisms will be discussed in the following paragraphs.

As mentioned in the previous section "Continuous tube with uniform diameter", a theoretical study suggested that differential growth between the epithelial sheet and the soft surrounding tissue can mechanically cause the formation of a tube with sinuous patterns (Fig. 8B). This is the case with the murine epididymal tubes and the trachea of Drosophila, where the soft surrounding tissues correspond to a mesenchymal layer and an extra-cellular matrix layer, respectively [115,116].

In the guts, the sinuous patterns are explained by differential growth between the tubes and the mesenteric membranes (Fig. 7C) [102]. Since the guts have smooth muscle layers, the longitudinal growth of the epithelial layers would be
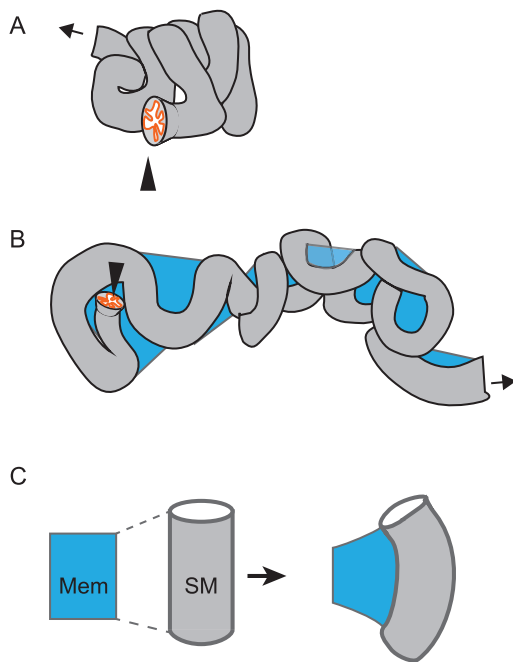
Figure 7 Sinuous shape of tubular organ. A. A compactly accommodated murine oviduct is illustrated. The entry from the ovary is shown by an arrowhead, and the exit to the uterus is shown by an arrow. B. An oviduct surgically disentangled is illustrated. A membrane (mesosalpinx; blue) is connecting to the tube. The tube exhibits a sinuous pattern. C. Differential growth between the tube and the membrane is explained. The membrane (blue) is connecting with the smooth muscle (SM) of the tube along the longitudinal direction of the tube. If the longitudinal length of the tube is longer than that of the membrane, the tube is deformed and possibly to form a sinuous pattern described in B.

Figure 8 Outcomes from differential growth of tissues. Outcomes of differential growth of tissues shown in Figures 4, 6, and 7 are summarized. A. In the presence of a stiff structure such as a smooth muscle layer (SM), differential growth between the tube and the epithelial sheet (Epi) results in the formation of epithelial folds. B. In the absence of a stiff structure, differential growth between the epithelial sheet (Epi) and the tube which is composed of softer extra cellular matrix or mesenchymal layer (EL) results in the formation of the non-uniform tube or of the sinuous tube. C. In the presence of the membrane (Mem) longitudinally binding to the tube, differential growth between the membrane and the tube results in the formation of the sinuous tube. Even in the case that the tube contains a stiff smooth muscle layer (SM), the membrane can deform the tube.

unable to deform the tubes. Alternatively, the mesenteric membranes have a critical role, which are tightly binding to the tubes along the longitudinal direction. Since the longitudinal growth of the tubes is rapider than that of the mesenteric membranes, the tubes are mechanically deformed, resulting in the formation of the sinuous patterns. This idea was both experimentally and theoretically validated [102], and a protein regulating the differential growth rate was also identified [103].

In the oviducts, it has not been examined how the sinuous patterns are generated. The oviducts have the smooth muscle layers similar to the guts. Moreover, there is a membrane longitudinally binding to the tube, called mesosalpinx (Fig. 7B). Therefore, the situation in the oviducts resembles to that in the gut, implying that the sinuous patterns in the oviducts is generated by differential growth between the membranes and the tubes (Fig. 8C). Experimental validations of the hypothesis including identification of proteins generating differential growth and measurements of stiffness of each tissue are important.
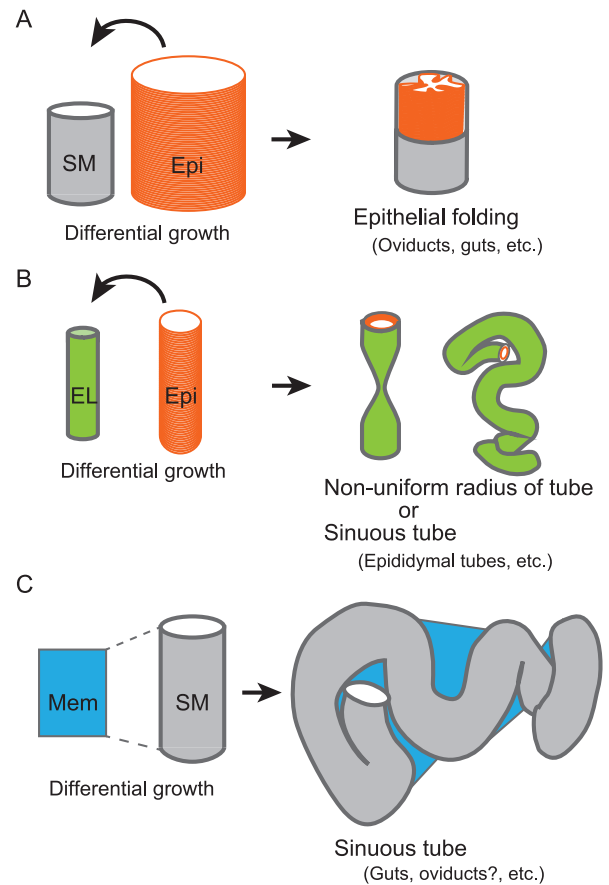
Impact of Differential Growth on Morphogenesis of Tubular Organs

As mentioned in the previous four sections, differential growth rate or length between adjacent tissues mechanically causes the formation of various structures in tubular organs. Here we summarize these structures and their formation. In the case that a luminal epithelial layer is longitudinally longer than a surrounding tissue, there can be two outcomes (Fig. 8). The first is that, if the surrounding tissue is stiff enough, the epithelial layer is deformed to form epithelial folds (Fig. 8A). This may be the case in the guts and the oviducts where the surrounding tissue is a smooth muscle layer [2,12]. The second is that, if the surrounding tissue is soft, the tube itself is deformed to form sinuous patterns

(Fig. 8B). This corresponds to the situation of the epididymal tubes where the surrounding tissue is a mesenchymal layer and that of the Drosophila tracheal tubes where the tissue is an extra-cellular matrix layer [115,116]. In addition, the diameters of the epididymal and tracheal tubes are too small to form folds in their luminal spaces. On the other hand, in the case that there is a membrane binding to a tubular organ along its longitudinal direction, differential growth between the membrane and the tube causes the formation of sinuous patterns of the tube (Fig. 8C). This is the case in the guts and probably in the oviducts [102]. In conclusion, differential growth or length among an epithelial layer, a surrounding tissue, and a binding membrane tissue is critical for the morphogenesis of tubular organs. Mathematical simulations considering stiffness of each tissue would provide information to judge the feasibilities of these hypotheses.

Egg Transportation

The mammalian oviducts can be divided into three sub-domains, infundibulum, ampulla and isthmus (Fig. 1A-i). Ovulated eggs are transported in this order towards uterus, and these sub-domains have different structure and function during the transportation [1,84,117].

In the entry of the mouse oviduct, infundibulum, large populations of epithelial cells are ciliated as mentioned in the section "Orchestrating cilia polarity" [11,84,118]. At the end of the oviduct (the entrance from the ovary), the epithelium is folded in an inside-out manner. Since each ovulated ovum is surrounded by cumulus cells and forming a large viscous structure called cumulus oocyte complex (COC), the COC can be easily transported into the oviduct once the COC touch the surface of the epithelium by the unidirectional ciliary beating [13]. Since the COC is a viscous structure, ciliary contact rather than the stream of oviduct fluid might play major roles in transportation (Fig. 9A).

Longitudinal epithelial fold might also help the transportation. The epithelial folds increase the surface area of epithelium, resulting in the increased probability of contact between the cilia and the COC. The structure of folds might make it possible to release the fluid pressure difference before and after the COC passes. According to our egg transportation experiments in cultured oviducts with longitudinally opened by surgical operation, the COCs are efficiently transported in the wild-type oviducts, whereas the COCs are wandering and stop their movement in the Celsr1 mutant oviducts [13][unpublished data]. Interestingly, in the wild-type oviducts, the COCs move along folds. In the Celsr1 mutant oviducts, when beads are used instead of the COCs, the beads accumulate around the branching sites of the folds. These facts imply the involvement of the folds and their shapes in efficient egg transportation, though mechanical explanations of these phenomena have not been established.

When COC are transported into the ampulla, COC will stay in the ampulla for several hours, waiting for the sperms
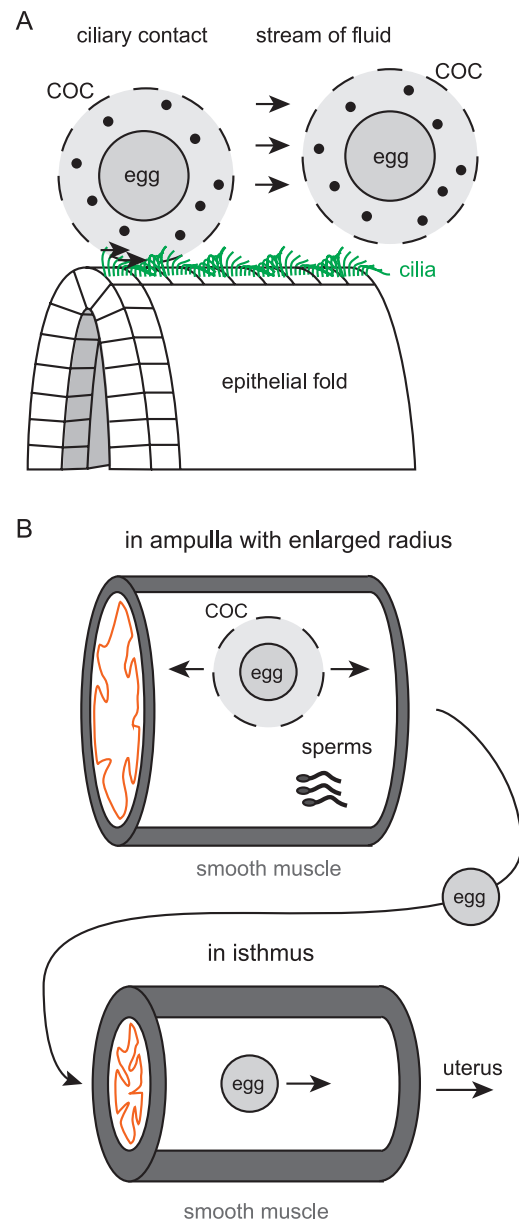

Figure 9 Egg transportation. A. Two possible mechanisms for egg transportation are described. Cilia directly contact to COCs to transport, or fluid flow generated by ciliary beating transports COCs. The structures of epithelial folds might be involved in transportation. Cilia are shown by green lines. Movements of COCs are described by arrows. Eggs are illustrated as gray circles in COCs. Cumulus cells are also shown by small black filled circles. B. Movements of COCs in ampulla and isthmus are illustrated. Smooth muscle contraction is involved in the forward and backward movements in the ampulla (arrows). In the ampulla, fertilization occurs. Sperms are also shown. The smooth muscle and a luminal epithelium are shown by gray and orange, respectively. Before entering the isthmus, the cumulus cells are removed. In the isthmus, eggs are transported by smooth muscle contraction.

coming from the uterus (Fig. 9B) [119]. During this stage, there are around 10 COCs in an ampulla, thus the ampulla is enlarged in the radius [12,119]. In the case of fertilization,

enzymes secreted from the sperms will degrade the hyaluronic acid connecting cumulus cells and the oocyte [119]. The radius of the isthmus is smaller than that of the ampulla, thus it is thought that the oocytes can enter the isthmus of the oviduct only after the COC is disassembled as COC is too large to get into the isthmus (Fig. 9B). However, this staying process is not fully mechanistically analyzed to the best of authors' knowledge. COCs or ova are also reported to go back and forth within the ampulla during staying, and this movement is supported by the muscle contraction (Fig. 9B) [120–123].

In the isthmus, smooth muscle layers are thicker compared to other sub-domains of the oviducts, and only around 10% of epithelial cells are ciliated in the epithelium [1,84,118]. Here, muscle contraction is supposed to play major roles in transportation (Fig. 9B), though the direct observation of the inside of the oviducts is hard to achieve. Recent technological advancement in tomography enables researcher to monitoring the inside of female reproductive tract from outside [124,125], which will make progress on uncovering how the ovum are actually transported.

Egg Shape Formation in Oviduct

Female reproductive tracts have a role in egg shape formation in some species such as birds and probably nematodes [126,127]. In these species, the eggs exhibit oval or elongated shapes but not sphere ones. Egg shape can affect embryogenesis [127,128]. Fertilized eggs in mice also show slightly elongated shapes which are critical for body axis formation [129,130], though it is unknown whether the oviducts affect the shapes. In this section, we introduce egg shape formation in birds to consider possible roles of the mammalian oviducts in egg shape formation.

In the avian oviducts, multiple segments namely infundibulum, magnum, isthmus and the uterus are seen anatomically, and a large number of folds along the longitudinal axis of the tube are also formed on the luminal surface. The female reproductive tract extending from the ovary to the uterus exists only on the left side of the body but not on the right side where the tract regresses to reduce body weight, which may be advantageous for flight [131].

The yolk on which blastodisc is located is released from the ovary. After fertilization, albumen (egg white), soft egg membrane and calcareous eggshell gather around the yolk in the oviduct. Fertilization occurs in the infundibulum, and a disc-shaped embryo located on surface of the yolk starts its development before the egg is laid from the cloaca. Reptile eggs are also covered by eggshells, but their shapes are spheres or ellipsoids (Fig. 10A). On the other hand, the shape of avian eggshells is "oval or ovoidal", which shows two axes of asymmetry with one pointed end and one blunt end (Fig. 10A). How is this ovoidal eggshell shape produced in the oviducts? A yolk travels through the oviduct while the yolk is surrounded by egg white at the magnum, and the
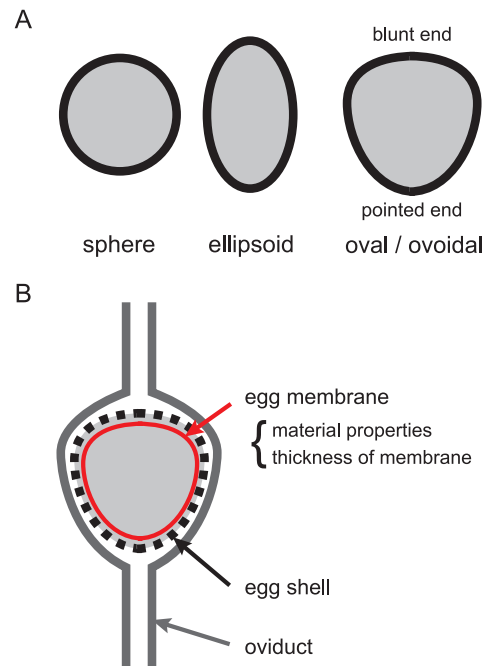

Figure 10 Avian egg shape. A. Avian and reptile eggs are illustrated. In reptiles, sphere and ellipsoidal shapes are observed. In birds, oval/ovoidal shapes are observed. B. Avian egg shapes are determined in the oviducts. The material properties and the thickness of egg membranes are involved in shaping the eggs.

shape of the egg is determined at the isthmus-uterus junction after the egg is covered by soft egg membrane [132]. Then calcified eggshell is formed in the uterus to follow the shape of the soft egg membrane. A lot of egg shapes in various bird species have been measured [126]. The shapes of the egg membranes may be evolutionarily related to the flight capability of birds [126]. The shapes can be modulated by the material properties and thickness of the egg membranes (Fig. 10B) [126]. The mechanical properties of the egg membranes are not uniform. Moreover, there are differences in pressure locally applied to the egg membrane surfaces, which are, at least partially, derived from mechanical forces applied from muscular contraction of the oviducts. In combination with these mechanical components, various egg shapes are formed.

As mentioned above, the shapes of eggs bearing egg shell are modified by the mechanical interaction between the eggs and the oviducts. In mammals, eggs don't have stiff egg shells but have relatively softer membranes called zona pellucida [129]. There is a possibility that the shapes of the zona pellucida or the COCs are modified by the mechanical interaction with the oviducts, though there have been neither experimental measurements of the shapes *in vivo* nor theoretical speculations.

Role of Oviduct and Egg Shape in Embryogenesis

The oviduct is a place where embryos experience their

first development. The oviduct can have potential roles in embryogenesis as well as egg shape modulation. The oviducts have biochemical or epigenetic roles in embryogenesis [133], whereas any mechanical roles have not been reported. In contrast, the avian oviducts mechanically contribute to embryogenesis with the combination of egg shapes and gravity as described below.

When "the egg" is laid from the hen's cloaca, an embryo locates on the top of yolk (Fig. 11A). The future anterior-posterior body axis is already specified in an embryo at this stage. When the chicken eggshell is opened with its pointed end to the right and the blunt end to the left, the most of embryos will develop perpendicularly to the longer axis of the egg, with its posterior end towards the observer (Fig. 11A) [134]. This relationship between the eggshell shape and the embryonic body axis is called "the rule of Von Bear". How is this rule established? There are several components to realize this rule. 1) One part of the egg yolk with blasto-disc (or the future embryo) is always located upward with respect to the direction of gravity (Fig. 11B, left panel). In other words, one side of the yolk with the embryo is lighter than the other side. In addition, the egg yolk is supported at two points by the chalazas, and the other ends of the chalazas are attached to the egg membrane at the edges of the long axis of the egg (Fig. 11B, left panel). The egg yolk is floating in the egg white, and it can rotate along the line between the two points where chalazas attach to the yolk (Fig. 11B, free rotation). By these conditions, the embryo always exists on the upper side in the egg membrane. 2) The pointed end of the egg is heading for the hen's cloaca or the downstream in the oviduct (Fig. 11B, left panel). 3) Most eggs are rotating in a constant clockwise direction along the circumferential direction of the oviduct in the uterus when seen from the downstream (Fig. 11B, right panel). By the combination of these components with the viscosity of egg whites, the embryo is maintained in an oblique position and one side of the embryo is kept in higher position (Fig. 11C, right panel) [135]. This higher region is coincided with the future posterior side (Fig. 11C, right panel) [136]. These strongly suggest that the gravity plays an important role for specification of future body axis in avian embryos, and the rotation of the egg in the oviduct contributes to establish this asymmetry. For the rotation of the egg, the oviduct or the uterus should mechanically interact with the egg. If the smooth muscle of the oviducts contracted in a chiral manner, this phenomenon could be explained. Epithelial folds and cilia could be also involved in, if they exhibited chiral orientation. Experimental observations, measurements, and mathematical simulations are needed to examine these possibilities.

In mammals, it is unknown whether the eggs rotate through the interaction with the oviducts, though the eggs are rotated by chiral beating of spermatozoa in a counterclockwise manner during fertilization [137]. More extensive observations of the dynamics of the eggs and the oviducts will be informative to understand the mechanical roles of the ovi-
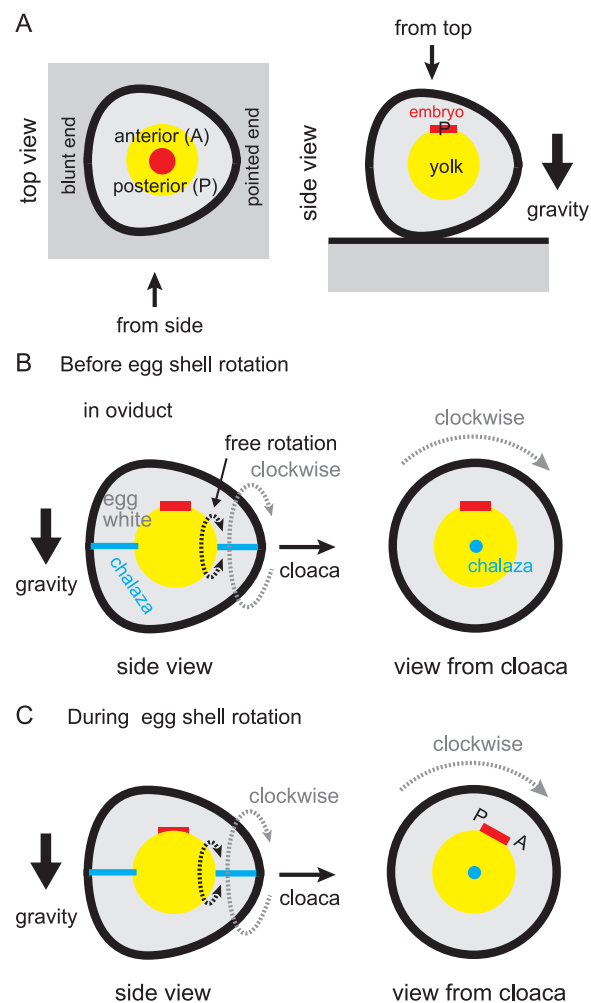

Figure 11   Role of egg shape and oviduct in body axis formation of avian embryo. A. The anterior-posterior axis of an embryo is explained in an avian egg. The embryo and the yolk are written by red and yellow, respectively. The top and side views are described. In the right panel, the posterior side is shown by P. B. An avian egg with an embryo in the oviduct is illustrated. The side view and the view from the cloaca are shown. Before the rotation of the egg shell, the embryo is located on the top of the yolk. C. The position of the embryo during the rotation of the egg shell is illustrated. The clockwise rotation of the egg shell exerts force on the yolk via the viscous egg white, leading to oblique positioning of the embryo (right panel). The upper side of the embryo will become posterior (P).

ducts in egg rotation as well as embryogenesis and egg transportation.

Perspectives

In this review, we have been discussing multiscale structures of the oviducts including the aligned cilia, the checkerboard pattern of epithelial cell distribution, the aligned epithelial folds, the continuity of the tube, etc. We discussed the mechanisms of how these structures are formed from the viewpoints of biophysics and biomechanics while considering similar structures observed in other organs. The

mechanisms involve dynamics of protein localization and of sub-cellular structures, differential cell adhesiveness, differential tissue growth, tissue stiffness, etc. Although recent cooperation among genetic and theoretical approaches has been advancing the understanding of the mechanisms, some of the mechanisms remain still obscure or hypothetical.

To fully understand the mechanisms underlying the formation of the structures above, *in vitro* reconstitution experiments are also useful. Localization of membrane proteins on a specific cell-cell boundary was reconstituted in purified systems [138]. Many researches have been trying to reconstitute PCP by using *in vitro* cultured cells. PCP ranging a few neighboring cells were formed *in vitro* [50,139], but it has not been succeeded to form PCP ranging a whole epithelial sheet. Therefore, it is suggested that there are unknown factors or conditions to completely form PCP. On the other hand, formation of cell distribution patterns was reconstituted based on the differential adhesion hypothesis [140,141], though it is still difficult to generate a beautiful checkerboard pattern. Unknown conditions including temporal regulation mimicking developmental processes might be considered to reconstitute cell distribution patterns and PCP. Various patterns of tissue folding in small tissues were generated *in vitro* [87]. However, tissue level reconstitution in large scale is still challenging.

Generating biological structures using artificial material is also helpful to understand the mechanisms for the formation of the structures. Tissue elongation, patterns formation of sinuous tubes, and folding in the brain etc. were artificially reconstructed by using metal beads, latex membranes, rubber tubes, swelling soft gels [73,96,102]. Robotics approaches may also be implicative to understand self-organizing cell behaviors [142]. Taken together, to fully understand the mechanisms for the formation of multiscale structures, multi-disciplinary approaches including genetics, theoretical modeling, synthetic biology, engineering using artificial materials, and robotics will become more and more important.

In this review, we also discussed the physiological functions of the oviducts in the context of the multiscale structures in this organ. The multiscale structures would be important for egg transportation in mammals, and possibly for egg shape formation and subsequent embryogenesis in birds. To achieve these physiological functions, in addition to the structures, it is necessary to consider fluid mechanics in the lumen, gravity, etc. The oviduct is a good example indicating the involvement of multiscale structures in physiological functions of an organ. Multiscale understanding of organs are still challenging especially in larger organs including most of mammalian organs. In the case of the heart, multiscale modeling and simulations about the heart physiologies have been developed, which would enable us to understand the relationship among molecules, sub-cellular structures, cells, and tissues [143,144]. These studies will lead to the comprehensive understanding of the physiologies of the heart. In the oviduct, the cilia, the epithelial folds, and

the smooth muscle contraction would be involved in egg transportation, however, it has not been established which dominantly contributes to the transportation. Multiscale knowledges would be clinically important. Some cases of infertility are derived from the oviducts. The infertility may be caused by defects in the cilia, the epithelial folds, or smooth muscle contraction. Closing of the tube should also cause the infertility. However, it is not well known which the major cause is. Collaborations among experimental studies, multiscale simulations, and clinical studies will be fruitful in both the basic biology and clinical fields.

Acknowledgements

Conflicts of interest

The authors declare no competing financial interests.

Author contributions

H. K., D. S., T. F. wrote the manuscript.

References

[1] Agduhr, E. Studies on the structure and development of the bursa ovarica and the tuba uterina in the mouse. *Acta Zool.* **8**, 1–133 (1927).

[2] Shyer, A. E., Tallinen, T., Nerurkar, N. L., Wei, Z., Gil, E. S., Kaplan, D. L., *et al.* Villification: how the gut gets its villi. *Science* **342**, 212–218 (2013).

[3] Wiggs, B. R., Hrousis, C. A., Drazen, J. M. & Kamm, R. D. On the mechanism of mucosal folding in normal and asthmatic airways. *J. Appl. Physiol.* **83**, 1814–1821 (1997).

[4] Li, B., Cao, Y. P. & Feng, X. Q. Growth and surface folding of esophageal mucosa: A biomechanical model. *J. Biomech.* **44**, 182–188 (2011).

[5] Yang, W., Fung, T. C., Chian, K. S. & Chong, C. K. Instability of the two-layered thick-walled esophageal model under the external pressure and circular outer boundary condition. *J. Biomech.* **40**, 481–490 (2007).

[6] Lambert, R. K., Codd, S. L., Alley, M. R. & Pack, R. J. Physical determinants of bronchial mucosal folding. *J. Appl. Physiol.* **77**, 1206–1216 (1994).

[7] Netter, F. H. *Atlas of Human Anatomy*. 5th ed. (Saunders, Philadelphia, 2010).

[8] "University hospital Medical Information Network (UMIN. ac.jp), Web Histology". http://plaza.umin.ac.jp/~web-hist/

[9] Ben Amar, M. & Jia, F. Anisotropic growth shapes intestinal tissues during embryogenesis. *Proc. Natl. Acad. Sci. USA* **110**, 10525–10530 (2013).

[10] Burgess, D. R. Morphogenesis of intestinal villi. II. Mecha-

nism of formation of previllous ridges. *J. Embryol. Exp. Morphol.* **34**, 723–740 (1975).

[11] Shi, D., Komatsu, K., Hirao, M., Toyooka, Y., Koyama, H., Tissir, F., *et al.* Celsr1 is required for the generation of polarity at multiple levels of the mouse oviduct. *Development* **141**, 4558–4568 (2014).

[12] Koyama, H., Shi, D., Suzuki, M., Ueno, N., Uemura, T. & Fujimori, T. Mechanical Regulation of Three-Dimensional Epithelial Fold Pattern Formation in the Mouse Oviduct. *Biophys. J.* **111**, 650–665 (2016).

[13] Shi, D., Komatsu, K., Uemura, T. & Fujimori, T. Analysis of ciliary beat frequency and ovum transport ability in the mouse oviduct. *Genes Cells* **16**, 282–290 (2011).

[14] Yang, Y. (ed) *Planar cell polarity during development, Volume 101 1st Edition. Curr. Top. Dev.* (Academic Press, 2012).

[15] Vladar, E. K., Antic, D. & Axelrod, J. D. Planar cell polarity signaling: the developing cell's compass. *Cold Spring Harb. Perspect. Biol.* **1**, a002964 (2009).

[16] Adler, P. N. The frizzled/stan pathway and planar cell polarity in the Drosophila wing. *Curr. Top. Dev. Biol.* **101**, 1–31 (2012).

[17] Usui, T., Shima, Y., Shimada, Y., Hirano, S., Burgess, R. W., Schwarz, T. L., *et al.* Flamingo, a Seven-Pass Transmembrane Cadherin, Regulates Planar Cell Polarity under the Control of Frizzled. *Cell* **98**: 585–595 (1999).

[18] Bastock, R., Strutt, H. & Strutt, D. Strabismus is asymmetrically localised and binds to Prickle and Dishevelled during Drosophila planar polarity patterning. *Development* **130**, 3007–3014 (2003).

[19] Axelrod, J. D. Unipolar membrane association of Dishevelled mediates Frizzled planar cell polarity signaling. *Genes Dev.* **15**, 1182–1187 (2001).

[20] Shi, D., Usami, F., Komatsu, K., Oka, S., Abe, T., Uemura, T., *et al.* Dynamics of planar cell polarity protein Vangl2 in the mouse oviduct epithelium. *Mech. Dev.* **141**, 78–89 (2016).

[21] Tree, D. R., Ma, D. & Axelrod, J. D. A three-tiered mechanism for regulation of planar cell polarity. *Semin. Cell Dev. Biol.* **13**, 217–224 (2002).

[22] Adler, P. N. The frizzled/stan pathway and planar cell polarity in the Drosophila wing. *Curr. Top. Dev. Biol.* **101**, 1–31 (2012).

[23] Butler, M. T. & Wallingford, J. B. Planar cell polarity in development and disease. *Nat. Rev. Mol. Cell Biol.* **18**, 375–388 (2017).

[24] Devenport, D. The cell biology of planar cell polarity. *J. Cell Biol.* **207**, 171–179 (2014).

[25] Strutt, H. & Strutt, D. Asymmetric localisation of planar polarity proteins: Mechanisms and consequences. *Semin. Cell Dev. Biol.* **20**, 957–963 (2009).

[26] Harumoto, T., Ito, M., Shimada, Y., Kobayashi, T. J., Ueda, H. R., Lu, B., *et al.* Atypical cadherins Dachsous and Fat control dynamics of noncentrosomal microtubules in planar cell polarity. *Dev. Cell* **19**, 389–401 (2010).

[27] Shimada, Y., Yonemura, S., Ohkura, H., Strutt, D. & Uemura, T. Polarized transport of Frizzled along the planar microtubule arrays in Drosophila wing epithelium. *Dev. Cell* **10**, 209–222 (2006).

[28] Ma, D., Yang, C. H., McNeill, H., Simon, M. A. & Axelrod, J. D. Fidelity in planar cell polarity signalling. *Nature* **421**, 543–547 (2003).

[29] Matis, M., Russler-Germain, D. A., Hu, Q., Tomlin, C. J. & Axelrod, J. D. Microtubules provide directional information for core PCP function. *Elife* **3**, e02893 (2014).

[30] Heck, B. W. & Devenport, D. Trans-endocytosis of Planar Cell Polarity Complexes during Cell Division. *Curr. Biol.* **27**, 3725–3733.e4 (2017).

[31] Sagner, A., Merkel, M., Aigouy, B., Gaebel, J., Brankatschk, M., Julicher, F., *et al.* Establishment of global patterns of pla-nar polarity during growth of the Drosophila wing epithelium. *Curr. Biol.* **22**, 1296–1301 (2012).

[32] Minegishi, K., Hashimoto, M., Ajima, R., Takaoka, K., Shinohara, K., Ikawa, Y., *et al.* A Wnt5 Activity Asymmetry and Intercellular Signaling via PCP Proteins Polarize Node Cells for Left-Right Symmetry Breaking. *Dev. Cell* **40**, 439–452.e4 (2017).

[33] Sepich, D. S., Usmani, M., Pawlicki, S. & Solnica-Krezel, L. Wnt/PCP signaling controls intracellular position of MTOCs during gastrulation convergence and extension movements. *Development* **138**, 543–552 (2011).

[34] Strutt, H., Warrington, S. J. & Strutt, D. Dynamics of core planar polarity protein turnover and stable assembly into discrete membrane subdomains. *Dev. Cell* **20**, 511–525 (2011).

[35] Chien, Y. H., Keller, R., Kintner, C. & Shook, D. R. Mechanical strain determines the axis of planar polarity in ciliated epithelia. *Curr. Biol.* **25**, 2774–2784 (2015).

[36] Kim, S. K., Shindo, A., Park, T. J., Oh, E. C., Ghosh, S., Gray, R. S., *et al.* Planar cell polarity acts through septins to control collective cell movement and ciliogenesis. *Science* **329**, 1337–1340 (2010).

[37] Shindo, A. & Wallingford, J. B. PCP and septins compartmentalize cortical actomyosin to direct collective cell movement. *Science* **343**, 649–652 (2014).

[38] Amonlirdviman, K., Khare, N. A., Tree, D. R., Chen, W. S., Axelrod, J. D. & Tomlin, C. J. Mathematical modeling of planar cell polarity to understand domineering nonautonomy. *Science* **307**, 423–426 (2005).

[39] Le Garrec, J. F., Lopez, P. & Kerszberg, M. Establishment and maintenance of planar epithelial cell polarity by asymmetric cadherin bridges: a computer model. *Dev. Dyn.* **235**, 235–246 (2006).

[40] Merkel, M., Sagner, A., Gruber, F. S., Etournay, R., Blasse, C., Myers, E., *et al.* The balance of prickle/spiny-legs isoforms controls the amount of coupling between core and fat PCP systems. *Curr. Biol.* **24**, 2111–2123 (2014).

[41] Aigouy, B., Farhadifar, R., Staple, D.B., Sagner, A., Röper, J. C., Jülicher, F., *et al.* Cell Flow Reorients the Axis of Planar Polarity in the Wing Epithelium of Drosophila. *Cell* **142**, 773–786 (2010).

[42] Szabó, B., Szöllösi, G., Gönci, B., Jurányi, Z., Selmeczi, D. & Vicsek, T. Phase transition in the collective migration of tissue cells: Experiment and model. *Phys. Rev. E Stat. Nonlin. Soft Matter Phys.* **74**, 061908 (2006).

[43] Li, X., Balagam, R., He, T.-F., Lee, P. P., Igoshin, O. A. & Levine, H. On the mechanism of long-range orientational order of fibroblasts. *Proc. Natl. Acad. Sci. USA* **114**, 8974–8979 (2017).

[44] Nagai, K. H. Collective motion of rod-shaped self-propelled particles through collision. *Biophys. Physicobiol.* **15**, 51–57 (2018).

[45] Halbert, S. A., Tam, P. Y. & Blandau, R. J. Egg transport in the rabbit oviduct: the roles of cilia and muscle. *Science* **191**, 1052–1053 (1976).

[46] Boisvieux-Ulrich, E., Laine, M. C. & Sandoz, D. The orientation of ciliary basal bodies in quail oviduct is related to the ciliary beating cycle commencement. *Biol. Cell* **55**, 147–150 (1985).

[47] Werner, M. E., Hwang, P., Huisman, F., Taborek, P., Yu, C. C. & Mitchell, B. J. Actin and microtubules drive differential aspects of planar cell polarity in multiciliated cells. *J. Cell Biol.* **195**, 19–26 (2011).

[48] Herawati, E., Taniguchi, D., Kanoh, H., Tateishi, K., Ishihara, S. & Tsukita, S. Multiciliated cell basal bodies align in stereotypical patterns coordinated by the apical cytoskeleton. *J. Cell Biol.* **214**, 571–586 (2016).

[49] Kunimoto, K., Yamazaki, Y., Nishida, T., Shinohara, K., Ishikawa, H., Hasegawa, T., *et al.* Coordinated ciliary beating requires Odf2-mediated polarization of basal bodies via basal feet. *Cell* **148**, 189–200 (2012).

[50] Vladar, E. K., Bayly, R. D., Sangoram, A. M., Scott, M. P. & Axelrod, J. D. Microtubules enable the planar cell polarity of airway cilia. *Curr. Biol.* **22**, 2203–2212 (2012).

[51] Tissir, F., Qu, Y., Montcouquiol, M., Zhou, L., Komatsu, K., Shi, D., *et al.* Lack of cadherins Celsr2 and Celsr3 impairs ependymal ciliogenesis, leading to fatal hydrocephalus. *Nat. Neurosci.* **13**, 700–707 (2010).

[52] Mitchell, B., Stubbs, J. L., Huisman, F., Taborek, P., Yu, C. & Kintner, C. The PCP pathway instructs the planar orientation of ciliated cells in the Xenopus larval skin. *Curr. Biol.* **19**, 924–929 (2009).

[53] Guirao, B., Meunier, A., Mortaud, S., Aguilar, A., Corsi, J. M., Strehl, L., *et al.* Coupling between hydrodynamic forces and planar cell polarity orients mammalian motile cilia. *Nat. Cell Biol.* **12**, 341–350 (2010).

[54] Mitchell, B., Jacobs, R., Li, J., Chien, S. & Kintner, C. A positive feedback mechanism governs the polarity and motion of motile cilia. *Nature* **447**, 97–101 (2007).

[55] You, Y., Richer, E. J., Huang, T. & Brody, S. L. Growth and differentiation of mouse tracheal epithelial cells: selection of a proliferative population. *Am. J. Physiol. Lung Cell. Mol. Physiol.* **283**, L1315-L1321 (2002).

[56] Prost, J., Jülicher, F. & Joanny, J. F. Active gel physics. *Nat. Phys.* **11**, 111-117 (2015).

[57] Marchetti, M. C., Joanny, J. F., Ramaswamy, S., Liverpool, T. B., Prost, J., Rao, M., *et al.* Hydrodynamics of soft active matter. *Rev. Mod. Phys.* **85**, 1143–1189 (2013).

[58] Elgeti, J. & Gompper, G. Emergence of metachronal waves in cilia arrays. *Proc. Natl. Acad. Sci. USA* **110**, 4470–4475 (2013).

[59] Gueron, S., Levit-Gurevich, K., Liron, N. & Blum, J. J. Cilia internal mechanism and metachronal coordination as the result of hydrodynamical coupling. *Proc. Natl. Acad. Sci. USA* **94**, 6001–6006 (1997).

[60] Osterman, N. & Vilfan, A. Finding the ciliary beating pattern with optimal efficiency. *Proc. Natl. Acad. Sci. USA* **108**, 15727–15732 (2011).

[61] Yamanaka, H. I. & Honda, H. A checkerboard pattern manifested by the oviduct epithelium of the Japanese quail. *Int. J. Dev. Biol.* **34**, 377–383 (1990).

[62] Steinberg, M. S. Reconstruction of Tissues by Dissociated Cells. *Science* **141**, 401–408 (1963).

[63] Steinberg, M. S. Differential adhesion in morphogenesis: a modern view. *Curr. Opin. Genet. Dev.* **17**, 1281–1286 (2007).

[64] Togashi, H., Kominami, K., Waseda, M., Komura, H., Miyoshi, J., Takeichi, M., *et al.* Nectins Establish a Checkerboard-Like Cellular Pattern in the Auditory Epithelium. *Science* **333**, 1144–1147 (2011).

[65] Walton, K. D., Whidden, M., Kolterud, Å., Shoffner, S., Czerwinski, M. J., Kushwaha, J., *et al.* Villification in the mouse: Bmp signals control intestinal villus patterning. *Development* **143**, 427–436 (2016).

[66] Ferri, S., Junqueira, L.C., Medeiros, L. F. & Mederios, L. O. Gross, microscopic and ultrastructural study of the intestinal tube of Xenodon merremii Wagler, 1824 (Ophidia). *J. Anat.* **121**, 291–301 (1976).

[67] Yamamoto, Y., Khamura, N., Yamada, J. & Yamashita, T. Three-dimensional architecture of the subepithelial connective tissue in the omasal laminae of sheep and cattle. *Acta Anat. (Basel)* **146**, 238–243 (1993).

[68] Banks, W. J. *Applied Veterinary Histology*. 3rd ed. (Mosby, Inc., St. Louis, Missouri, 1993).

[69] Li, S., Kato, A., Takabe, S., Chen, A., Romero, M. F., Umezawa, T., *et al.* Expression of a novel isoform of Na+/H+ exchanger 3 in the kidney and intestine of banded houndshark, Triakis scyllium. *Am. J. Physiol. Regul. Integr. Comp. Physiol.* **304**, R865–R876 (2013).

[70] Koyama, H. & Fujimori, T. Biomechanics of epithelial fold pattern formation in the mouse female reproductive tract. *Curr. Opin. Genet. Dev.* **51**, 59–66 (2018).

[71] Varner, V. D., Voronov, D. A. & Taber, L. A. Mechanics of head fold formation: investigating tissue-level forces during early development. *Development* **137**, 3801–3811 (2010).

[72] Khan, Z., Wang, Y., Wieschaus, E. F. & Kaschube, M. Quantitative 4D analyses of epithelial folding during Drosophila gastrulation. *Development* **141**, 2895–2900 (2014).

[73] Tallinen, T., Chung, J. Y., Rousseau, F., Girard, N. Lefèvre, J. & Mahadevan, L. On the growth and form of cortical convolutions. *Nat. Phys.* **12**, 588–593 (2016).

[74] Inoue, Y., Suzuki, M., Watanabe, T., Yasue, N., Tateo, I., Adachi, T., *et al.* Mechanical roles of apical constriction, cell elongation, and cell migration during neural tube formation in Xenopus. *Biomech. Model. Mechanobiol.* **15**, 1733–1746 (2016).

[75] Nishimura, T., Honda, H. & Takeichi, M. Planar cell polarity links axes of spatial dynamics in neural-tube closure. *Cell* **149**, 1084–1097 (2012).

[76] Koyama, H., Shi, D. & Fujimori, T. Role of mechanical force in fold pattern formation in oviduct. *Seibutsu Butsuri* **57**, 259–261 (2017).

[77] Huang, Z. Y., Hong, W. & Suo, Z. Nonlinear analyses of wrinkles in a film bonded to a compliant substrate. *J. Mech. Phys. Solids* **53**, 2101–2118 (2005).

[78] Ciarletta, P. & Ben Amar, M. Pattern formation in fiber-reinforced tubular tissues: Folding and segmentation during epithelial growth. *J. Mech. Phys. Solids* **60**, 525–537 (2012).

[79] Hannezo, E., Prost, J. & Joanny, J. F. Instabilities of mono-layered epithelia: Shape and structure of villi and crypts. *Phys. Rev. Lett.* **107**, 078104 (2011).

[80] Tallinen, T. & Biggins, J. S. Mechanics of invagination and folding : Hybridized instabilities when one soft tissue. *Phys. Rev. E Stat. Nonlin. Soft Matter Phys.* **92**, 022720 (2015).

[81] Bakst, M. R. Structure of the avian oviduct with emphasis on sperm storage in poultry. *J. Exp. Zool.* **282**, 618–626 (1998).

[82] Girling, J. E. The reptilian oviduct: A review of structure and function and directions for future research. *J. Exp. Zool.* **293**, 141–170 (2002).

[83] Wake, M. H. & Dickie, R. Oviduct Structure and Function and Reproductive Modes in Amphibians. *J. Exp. Zool.* **282**, 477–506 (1998).

[84] Stewart, C. A. & Behringer, R. R. Mouse oviduct development. *Results Probl. Cell Differ.* **55**, 247–262 (2012).

[85] Suzuki, M., Sato, M., Koyama, H., Hara, Y., Hayashi, K., Yasue, N., *et al.* Distinct intracellular Ca^{2+} dynamics regulate apical constriction and differentially contribute to neural tube closure. *Development* **144**, 1307–1316 (2017).

[86] Heer, N. C., Miller, P. W., Chanet, S., Stoop, N., Dunkel, J. & Martin, A. C. Actomyosin-based tissue folding requires a multicellular myosin gradient. *Development* **144**: 1876–1886 (2017).

[87] Hughes, A. J., Miyazaki, H., Coyle, M. C., Zhang, J., Laurie, M. T., Chu, D., *et al.* Engineered Tissue Folding by Mechanical Compaction of the Mesenchyme Article Engineered Tissue Folding by Mechanical Compaction of the Mesenchyme. *Dev. Cell* **44**, 165–178.e6 (2018).

[88] Lecuit, T., Lenne, P.-F. & Munro, E. Force Generation, Transmission, and Integration during Cell and Tissue Morphogenesis. *Annu. Rev. Cell Dev. Biol.* **27**, 157–184 (2011).

[89] Xiong, F., Ma, W., Hiscock, T. W., Mosaliganti, K. R., Tentner,

A. R., Brakke, K. A., *et al.* Interplay of Cell Shape and Division Orientation Promotes Robust Morphogenesis of Developing Epithelia. *Cell* **159**, 415–427 (2014).

[90] Sugimura, K. & Ishihara, S. The mechanical anisotropy in a tissue promotes ordering in hexagonal cell packing. *Development* **140**, 4091–4101 (2013).

[91] Tamada, M. & Zallen, J. A. Square Cell Packing in the Drosophila Embryo through Spatiotemporally Regulated EGF Receptor Signaling. *Dev. Cell* **35**, 151–161 (2015).

[92] Etournay, R., Popovic, M., Merkel, M., Nandi, A., Blasse, C., Aigouy, B., *et al.* Interplay of cell dynamics and epithelial tension during morphogenesis of the Drosophila pupal wing. *Elife* **4**, e07090 (2015).

[93] Condic, M. L., Fristrom, D. & Fristrom, J.W. Apical cell shape changes during Drosophila imaginal leg disc elongation: a novel morphogenetic mechanism. *Development* **111**, 23–33 (1991).

[94] Jiang, D. & Smith, W. C. Ascidian notochord morphogenesis. *Dev. Dyn.* **236**, 1748–1457 (2007).

[95] Nelson, K. S., Khan, Z., Molnár, I., Mihály, J., Kaschube, M. & Beitel, G. J. Drosophila Src regulates anisotropic apical surface growth to control epithelial tube size. *Nat. Cell Biol.* **14**, 518–525 (2012).

[96] Imuta, Y., Koyama, H., Shi, D., Eiraku, M., Fujimori, T. & Sasaki, H. Mechanical control of notochord morphogenesis by extra-embryonic tissues in mouse embryos. *Mech. Dev.* **132**, 44–58 (2014).

[97] Ishihara, S. & Sugimura, K. Bayesian inference of force dynamics during morphogenesis. *J. Theor. Biol.* **313**, 201–211 (2012).

[98] Strutt, D. I., Weber, U. & Mlodzik, M. The role of RhoA in tissue polarity and Frizzled signalling. *Nature* **387**, 292–295 (1997).

[99] Taniguchi, K., Maeda, R., Ando, T., Okumura, T., Nakazawa, N., Hatori, R., *et al.* Chirality in planar cell shape contributes to left-right asymmetric epithelial morphogenesis. *Science* **333**, 339–341 (2011).

[100] Song, H., Mak, K. K., Topol, L., Yun, K., Hu, J., Garrett, L., *et al.* Mammalian Mst1 and Mst2 kinases play essential roles in organ size control and tumor suppression. *Proc. Natl. Acad. Sci. USA* **107**, 1431–1436 (2010).

[101] Kunimoto, K., Bayly, R. D., Vladar, E. K., Vonderfecht, T., Gallagher, A.-R. & Axelrod, J. D. Disruption of Core Planar Cell Polarity Signaling Regulates Renal Tubule Morphogenesis but Is Not Cystogenic. *Curr. Biol.* **27**, 3120–3131 (2017).

[102] Savin, T., Kurpios, N. A., Shyer, A. E., Florescu, P., Liang, H., Mahadevan, L., *et al.* On the growth and form of the gut. *Nature* **476**, 57–62 (2011).

[103] Nerurkar, N. L., Mahadevan, L. & Tabin, C. J. BMP signaling controls buckling forces to modulate looping morphogenesis of the gut. *Proc. Natl. Acad. Sci. USA* **114**, 2277–2282 (2017).

[104] Gudipaty, S. A., Lindblom, J., Loftus, P. D., Redd, M. J., Edes, K., Davey, C. F., *et al.* Mechanical stretch triggers rapid epithelial cell division through Piezo1. *Nature* **543**, 118–121 (2017).

[105] Marinari, E., Mehonic, A., Curran, S., Gale, J., Duke, T. & Baum, B. Live-cell delamination counterbalances epithelial growth to limit tissue overcrowding. *Nature* **484**, 542–545 (2012).

[106] Eisenhoffer, G. T., Loftus, P. D., Yoshigi, M., Otsuna, H., Chien, C.-B., Morcos, P. A., *et al.* Crowding induces live cell extrusion to maintain homeostatic cell numbers in epithelia. *Nature* **484**, 546–549 (2012).

[107] Montel, F., Delarue, M., Elgeti, J., Malaquin, L., Basan, M., Risler, T., *et al.* Stress Clamp Experiments on Multicellular Tumor Spheroids. *Phys. Rev. Lett.* **107**, 188102 (2011).

[108] Nonomura, K., Woo, S., Chang, R. B., Gillich, A., Qiu, Z., Francisco, A. G., *et al.* Piezo2 senses airway stretch and mediates lung inflation-induced apnoea. *Nature* **541**, 176–181 (2017).

[109] Dupont, S., Morsut, L., Aragona, M., Enzo, E., Giulitti, S., Cordenonsi, M., *et al.* Role of YAP/TAZ in mechanotransduction. *Nature* **474**, 179–183 (2011).

[110] Sawada, Y., Tamada, M., Dubin-thaler, B. J., Cherniavskaya, O., Sakai, R., Tanaka, S., *et al.* Force Sensing by Mechanical Extension of the Src Family Kinase Substrate p130Cas. *Cell* **127**, 1015–1026 (2006).

[111] Vandenberg, A. L. & Sassoon, D. A. Non-canonical Wnt signaling regulates cell polarity in female reproductive tract development via van gogh-like 2. *Development* **136**, 1559–1570 (2009).

[112] Hannezo, E., Prost, J. & Joanny, J. F. Mechanical instabilities of biological tubes. *Phys. Rev. Lett.* **109**, 018101 (2012).

[113] Huang, C. C., Orvis, G. D., Kwan, K. M. & Behringer, R. R. Lhx1 is required in Müllerian duct epithelium for uterine development. *Dev. Biol.* **389**, 124–136 (2014).

[114] Orvis, G. D. & Behringer, R. R. Cellular mechanisms of Müllerian duct formation in the mouse. *Dev. Biol.* **306**, 493–504 (2007).

[115] Hirashima, T. Pattern Formation of an Epithelial Tubule by Mechanical Instability during Epididymal Development. *Cell Rep.* **9**, 866–873 (2014).

[116] Dong, B., Hannezo, E. & Hayashi, S. Balance between apical membrane growth and luminal matrix resistance determines epithelial tubule shape. *Cell Rep.* **7**, 941–950 (2014).

[117] Lyons, R. A., Saridoqan, E. & Djahanbakhch, O. The reproductive significance of human Fallopian tube cilia. *Hum. Reprod. Update* **12**, 363–372 (2006).

[118] Yamanouchi, H., Umezu, T. & Tomooka, Y. Reconstruction of oviduct and demonstration of epithelial fate determination in mice. *Biol. Reprod.* **82**, 528–533 (2010).

[119] Behringer, R. R., Gertsenstein, M., Nagy, K. V. & Nagy, A. *Manipulating the Mouse Embryo: A Laboratory Manual* (Cold Spring Harbor Laboratory Press, New York, 2014).

[120] Halbert, S. A., Becker, D. R. & Szal, S. E. Ovum transport in the rat oviductal ampulla in the absence of muscle contractility. *Biol. Reprod.* **40**, 1131–1136 (1989).

[121] Halbert, S. A., Tam, P. Y. & Blandau, R. J. Egg transport in the rabbit oviduct: the roles of cilia and muscle. *Science* **191**, 1052–1053 (1976).

[122] Blandau, R. J. *Gamete transport: comparative aspects in The Mammalian Oviduct Comparative Biology And Methodology* (University of Chicago Press, Chicago, 1969).

[123] Shi, D., Komatsu, K. & Fujimori, T. The physiology of the fallopian tube. The collection of ovum and the transport of fertilized eggs. *Clin. Gynecol. Obstet.* **70**, 810–816 (2016).

[124] Wang, S. & Larina, I. V. *In vivo* three-dimensional tracking of sperm behaviors in the mouse oviduct. *Development* **145**, dev157685 (2018).

[125] Vue, Z., Gonzalez, G., Stewart, C. A., Mehra, S. & Behringer, R. R. Volumetric imaging of the developing prepubertal mouse uterine epithelium using light sheet microscopy. *Mol. Reprod. Dev.* **85**, 397–405 (2018).

[126] Stoddard, M. C., Yong, E. H., Akkaynak, D., Sheard, C. & Tobias, J. A., Mahadevan, L. Avian egg shape: Form, function, and evolution. *Science* **356**, 1249–1254 (2017).

[127] Yamamoto, K. & Kimura, A. An asymmetric attraction model for the diversity and robustness of cell arrangement in nematodes. *Development* **144**, 4437–4449 (2017).

[128] Edgar, L., Wolf, N. & Wood, W. Early transcription in Caenorhabditis elegans embryos. *Development* **120**, 443–451 (1994).

[129] Kurotaki, Y., Hatta, K., Nakao, K., Nabeshima, Y.-I. & Fujimori, T. Blastocyst axis is specified independently of early cell lineage but aligns with the ZP shape. *Science* **316**, 719–723 (2007).

[130] Honda, H., Motosugi, N., Nagai, T., Tanemura, M. & Hiiragi, T. Computer simulation of emerging asymmetry in the mouse blastocyst. *Development* **135**, 1407–1414 (2008).

[131] Guioli, S., Nandi, S., Zhao, D., Burgess-Shannon, J., Lovell-Badge, R. & Clinton, M. Gonadal asymmetry and sex determination in birds. *Sex. Dev.* **8**, 227–242 (2014).

[132] Mao, K. M., Sultana, F., Howlider, M. A., Iwasawa, A. & Yoshizaki, N. The Magnum-Isthmus Junction of the Fowl Oviduct Participates in the Formation of the Avian-type Shell Membrane. *Zool. Sci.* **23**, 41–47 (2006).

[133] Li, S. & Winuthayanon, W. Oviduct: Roles in fertilization and early embryo development. *J. Endocrinol.* **232**, R1–R26 (2017).

[134] von Baer, K. E. Entwiklungsgeschichte des Hünchens im Eie. *Bonnträger, Königsb.* **315** (1828).

[135] VINTEMBERGER, P. & CLAVERT, J. On the determinism of bilateral symmetry in birds. XIII. The factors in the orientation of the embryo in relation to the axis of the egg and von Baer's rule, in the light of our controlled orientation experiments on the hen egg extracted from the uterus. *C. R. Seances Soc. Biol. Fil.* **154**, 1072–1076 (1960).

[136] Kochav, S. & Eyal-Giladi, H. Bilateral symmetry in chick embryo determination by gravity. *Science* **171**, 1027–1029 (1971).

[137] Ishimoto, K., Ikawa, M. & Okabe, M. The mechanics clarifying counterclockwise rotation in most IVF eggs in mice. *Sci. Rep.* **7**, 43456 (2017).

[138] Schmid, E. M., Bakalar, M. H., Choudhuri, K., Weichsel, J., Ann, H. S., Geissler, P.L., *et al.* Size-dependent protein segregation at membrane interfaces. *Nat. Phys.* **12**, 704–711 (2016).

[139] Aw, W. Y., Heck, B. W., Joyce, B. & Devenport, D. Transient Tissue-Scale Deformation Coordinates Alignment of Planar Cell Polarity Junctions in the Mammalian Skin. *Curr. Biol.* **26**, 2090–2100 (2016).

[140] Duguay, D., Foty, R. A. & Steinberg, M. S. Cadherin-mediated cell adhesion and tissue segregation: qualitative and quantitative determinants. *Dev. Biol.* **253**, 309–323 (2003).

[141] Toda, S., Blauch, L. R., Tang, S. K. Y., Morsut, L. & Lim, W. A. Programming self-organizing multicellular structures with synthetic cell-cell signaling. *Science* **361**, 156–162 (2018).

[142] Umedachi, T., Kitamura, T., Nakagaki, T., Kobayashi, R. & Ishiguro, A. A modular robot driven by protoplasmic streaming. *Proc. DARS2008* 193–202 (2008).

[143] Sugiura, S., Washio, T., Hatano, A., Okada, J., Watanabe, H. & Hisada, T. Multi-scale simulations of cardiac electrophysiology and mechanics using the University of Tokyo heart simulator. *Prog. Biophys. Mol. Biol.* **110**: 380–389 (2012).

[144] Hisada, T. "Multiscale & Multiphysics UT Heart Simulator". http://www.sml.k.u-tokyo.ac.jp/index.html